Universiteit Utrecht

Faculteit Bètawetenschappen

Debye Institute

Soft Condensed Matter Group

Particle tracking and analysis of depletion induced self assembly of colloidal rods

Bachelor Thesis

Dido Denier van der Gon

Natuur- en Sterrenkunde

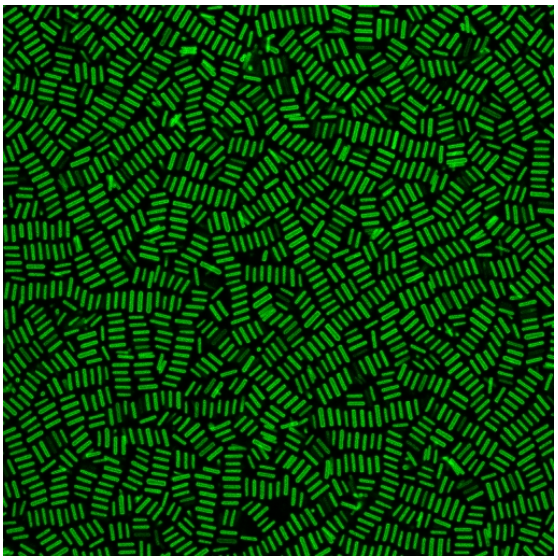

Supervisors:

Fabian Hagemans

Universiteit Utrecht

Prof. Dr. Alfons van Blaaderen

Universiteit Utrecht

Dr. Arnout Imhof

Universiteit Utrecht

June 2017

Contents

1 Introduction **3**

2 Theory **4**
2.1 Colloids . . . 4
2.2 Interactions . . . 4
2.2.1 Van der Waals interactions . . . 4
2.2.2 Double layer interaction . . . 5
2.2.3 DLVO interaction . . . 6
2.2.4 Depletion interaction . . . 7
2.3 Liquid crystals . . . 10
2.4 Order parameters . . . 12
2.4.1 Nematic order parameter . . . 12
2.4.2 Smectic order parameter . . . 12
2.5 Sedimentation . . . 13
2.6 Imaging . . . 13

3 Experimental **15**
3.1 Synthesis . . . 15
3.1.1 Rod synthesis . . . 15
3.1.2 Depletant synthesis . . . 16
3.2 Imaging . . . 17
3.2.1 Making the sample . . . 17
3.2.2 Acquiring the images . . . 17
3.2.3 Rod tracking . . . 18
3.3 Analysis . . . 18

4 Results and Discussion **19**
4.1 Rod and depletant synthesis . . . 19
4.2 Influence of the depletant in monolayers . . . 20
4.3 Influence of the depletant in sediments . . . 20
4.4 Tracking and analysing small sediments . . . 23
4.5 Tracking and analysing large sediments . . . 26
4.5.1 Difference in particle numbers between the samples after one day and after three weeks and between the different samples . . . 31
4.6 Dynamics . . . 31

5 Conclusion **33**

6 Outlook **34**

7 Acknowledgements **34**

Appendices **36**

A Mathematica notebook **36**

B Microscope settings **40**

Abstract

To get a good understanding of the depletion interaction acting on hard rods we present the tracking and analysing on the single particle level of the self assembly of silica rods made attractive using a depletant. Silica rods and spheres were successfully synthesised. Sediments with different volume fraction of these particles were made and imaged. Using a rod tracking code the locations and orientations of the rods were determined. By analysing this data we obtained the amount of order achieved within different samples. We saw that optima in depletion % (v/v) and pressure can be found. Also the amount of depletant needed depends on the size ratio rods:depletant. The dynamics of the system have also been studied showing the timescale on which the depletant interaction acts, after five minutes clustered particles were visible.

1 Introduction

Colloids are defined as particles dispersed in a medium with a diameter between 1 nm and 1 μm in at least one direction. [1] Idealised colloids are described by the Hard Sphere potential. This means that there are no long distance interactions between the colloids and that they cannot overlap. The potential is given by:

$$V(x) = \begin{cases} \infty \text{ if } x < r \\ 0 \quad \text{if } x > r \end{cases} \tag{1}$$

Where V is the potential and r the radius of the particles. Colloids exist in a great variety of shapes, such as spheres [2], nanotubes [3], barbels [4] and cubes [5]. A different shape results in a different phase behaviour. Spheres are isotropic particles, they are the same in all directions. On the contrary, anisotropic particles can have an orientation. A well known example are rod-shaped particles, the particles can exhibit orientational and / or positional order. This extra degree of freedom results in a phase that is neither a crystal nor a liquid and is therefore called a liquid crystal. [6] Most colloids are repulsive due to electrical charges. The behaviour of these rods has been widely studied and has led to the discovery of the liquid crystals mentioned earlier. [7] But what happens when these particles become attractive?

Colloids can be made attractive using a depletant. A depletant consists of small non-adsorbing particles, much smaller than the colloids you want to be attractive, dispersed in the medium. These small particles induce an attractive potential in the rods by augmenting their entropy. A lot of studies has already been done regarding rod like particles under depletion. Considering rods with a low aspect ratio it has been shown that polymers (the depletant) can cause a depletion attraction between bacteria (E. Coli cells, the rods), which can explain several natural phenomena. [8] Looking at rods with mixed aspect ratios a depletant has been used to divide nanorods in a suspension into fractions of equal aspect ratios. This method can be used for fractionation of any kind of nanoparticle dispersion. [9] Depletion in combination with high aspect ratio rods can be used to create stable 2D membranes which are one rod length thick from a solution of depleting polymers and hard rods. [10] Depletion has also been used to show the phase transition from nematic droplets to isotropic droplets. A nematic droplet is a droplet consisting of rod-like particles which are orientationally ordered but show no positional order. The isotropic droplets achieved consist of the same particles but shows zero order. This experiment shows how a depletant can be used to order rod-like colloids in a droplet. [11] These few examples give an idea of the numerous applications of the combination of hard rods of different aspect ratios and depletant. But the self assembly of rods made attractive using the depletion potential has not yet been studied extensively on the single particle level. The goal of this thesis is to study the influence of the depletion interaction on a system of rods on the single particle level by the means of particle tracking. And to give a measure of the order found in different systems using the data found by tracking the particles.

In this thesis tracking and analysing of the self assembly of rods in combination with a depletant are described. First, the theory necessary to understand the experiments will be described. This includes the properties of of colloids, the different interactions determining the behaviour of the rods, liquid crystals, how to determine the amount of order in a sample, the influence of sedimentation and how to image these particles. Then, I will describe the experimental methods used to perform the experiments, including the synthesis of both rods and depletant and how to image and analyse the samples. Afterwards, I will describe and discuss the results of the experiments. Finally a conclusion will be drawn from the experiments done.

2 Theory

2.1 Colloids

If the sedimentation of particles can be neglected in comparison to their thermal energy, particles are said to undergo Brownian motion.[12] This Brownian motion is caused by molecular agitation. The molecules or atoms "bump" into the colloids from different sides. Thus creating a net force in one direction, making the particle move. The result of these collisions is a random walk of the colloidal particle. [13]

The sedimentation velocity of the particles depends on various variables like density of the solvent and of the particle itself. The length scale at which there is an equilibrium between the thermal energy and the sedimentation is called the gravitational or sedimentation length. The gravitational length is defined as $l_{sed} = \frac{k_b T}{m_b g}$, where k_b is the Boltzmann constant, T the temperature, m_b the buoyant mass (the difference between the density of the particle and the solvent) and g the standard gravity. The gravitational length must be larger than the radius of the particle in order for the particles to "float". In table 1 the gravitational lengths for silica particles with a density of 2 g/cm^3 of different radii are given.

Radius/length in nm	l_{sed}
10/10	53.5 m
100/100	0.053 m
1000/1000	0.53 µm
100/800	4.4 mm
100/1000	3.5 mm
100/1500	0.23 mm

Table 1: The gravitational length for spherical and rod-like silica particles of different radii and lengths in a DMSO-water solution.

2.2 Interactions

To describe the interactions in a system consisting of both colloids and depletant various terms contribute to the total potential. The total potential will be the sum of the van der Waals, Double Layer and depletion interaction. These three potentials will be discussed below.

2.2.1 Van der Waals interactions

The London-Van der Waals forces are induced by dipole moments in all atoms and molecules. The constantly moving electrons in these atoms induce a constantly changing dipole moment. These dipole moments interact with those of other nearby atoms resulting in an attractive force on the order of R^{-6}. [14]

The strength of the Van der Waals attraction of colloidal particles (called the colloidal Van der Waals attraction) depends on the dielectric properties of the colloids as well as those of the

background medium. The potential as a function of h is shown in figure 2.

$$W_{vdw}(h) = -\frac{A}{6} f\left(\frac{h}{R}\right) \tag{2}$$

Where W_{VdW} is the Van der Waals attraction, A the Hamaker constant which usually is on the order of $10^{-19} - 10^{-21} J$ and $f(h/R)$ a function of h the closest distance between the surfaces of the two spheres and R the radii of the spheres, given by:

$$f(h/R) = \frac{2R^2}{h^2 + 4Rh} + \frac{2R^2}{h^2 + 4Rh + R^2} + \ln\left(\frac{h^2 + 4Rh}{h^2 + 4Rh + R^2}\right) \tag{3}$$

You can see that for small h the Van der Waals interaction is very strong. So a strong repulsion is needed in order to prevent the particles from aggregating.

The Hamaker constant for a colloidal dispersion in terms of the refractive index (n) and the dielectric constant (ϵ) is given by:[15]

$$A = \frac{3K_bT}{4}\left(\frac{\epsilon_p - \epsilon_s}{\epsilon_p + \epsilon_s}\right)^2 + \frac{3h\,\nu_e}{16\sqrt{2}}\frac{(n_p - n_s)^2}{(n_p + n_s)^{3/2}} \tag{4}$$

With ϵ_p and ϵ_s the dielectric constant of the particles and the solvent, h the Planck constant, ν_e the plasma frequency of the free electron gas and n_p and n_s the refractive indices of the particles and solvent respectively. Using the relation, $n = \sqrt{\epsilon/\epsilon_0}$ between the refractive index and the dielectric constant, where ϵ_0 is the dielectric constant of a vacuum. It can be shown that for n_p equals n_s the Hamaker constant becomes zero and thus the Van der Waals force becomes zero. [16]

2.2.2 Double layer interaction

The repulsion needed to prevent the particles from aggregating is often described by the Double layer interaction. Consider an electrical double layer around the particles, see figure 1. When the two double layers do not overlap there will be no interaction between the two particles. But as soon as the double layers start to overlap a repulsion will be induced by the equal charges. The size of the double layer can be tuned by the concentration of ions in the solvent. The distance at which two particles start to experience this repulsion is $2d$. This distance is referred to as the Debye screening length, which depends on the salt number density (n_s) and the Bjerrum length. The Bjerrum length is the distance at which the electrical interactions are of the same scale as the thermal energy: $l_b = \frac{e^2}{4\pi\epsilon k_b T}$ where e is the charge of an electron and $\epsilon = \epsilon_0\epsilon_r$, the permittivity. The Debye screening length is given by:

$$\kappa^{-1} = \frac{1}{\sqrt{8\pi l_b n_s}} \tag{5}$$

The double layer interaction depends on the (smallest) distance between the two particles and their double layers. It is given by the following function where B is the surface charge density of the colloids and normally in the range of 1-8 K_bT. [12] The function is shown in figure 2.

$$W_{DL}(h) = \frac{BR}{l_b} e^{h\kappa} \tag{6}$$

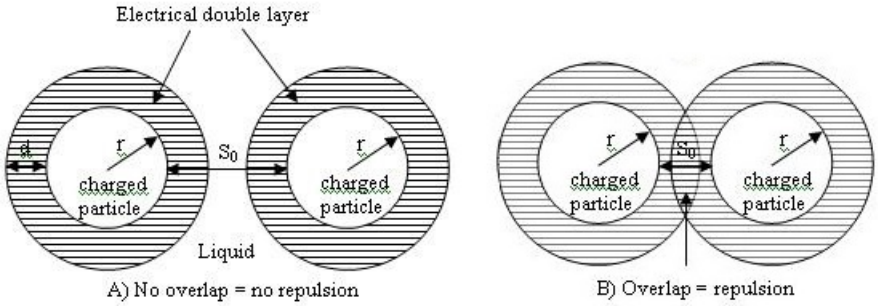

Figure 1: When two colloids get close together the electric double layers start to overlap thus resulting in a replusion.[17]

A more theoretical way of deriving the double layer potential is given by Verwey and Overbeek. Combining Poissons equation [1] with Boltzmanns theorem, which states that the average concentration of ions in the solvent can be calculated using the average value of the electric potential. Using the facts that it is of minor importance whether the ions have the same or opposite charges as the colloids and the fact that the electric potential is very small, the Boltzmann theorem can be rewritten in the form:

$$\rho = -2ne^2v^2\psi/kT \tag{7}$$

With ρ the density, n the the number of ions per cm^3, v the valency of the ions and ψ the electric potential. Combining these two equation and using the definition of the debye length, for small values of ψ we get the differential equation: [18]

$$\psi = \kappa^2\psi \tag{8}$$

Solving this equation for ψ gives the screened Yukawa-Coulomb potential: $\psi = \psi_0 \frac{a}{r}\mathrm{Exp}[\kappa(a-r)]$, with a the radius of the colloid. However, in the case of overlapping double layers a better approximation is given by Verwey and Overbeek: [18]

$$W_{DL} = \pi\,\epsilon_0\,\epsilon\,a\,\psi_0^2\,\frac{\mathrm{Exp}[\kappa(a-r]}{r/a} \tag{9}$$

We now have two descriptions of the double layer potential. An experimental expression given by equation 6 and a more theoretical expression given by equation 9.

2.2.3 DLVO interaction

The DLVO potential, named after Derjaguin, Landau, Verwey and Overbeek, is the most commonly used potential to describe the behaviour of colloids. It is a combination of the attractive Van der Waals Force and the Repulsive double layer interaction, see figure 2. This is the most commonly used potential to describe the behaviour of colloids in a medium.

$$W_{DLVO} = W_{VdW} + W_{DL} \tag{10}$$

[1] $\Delta\psi = -(4\pi\rho)/\epsilon$

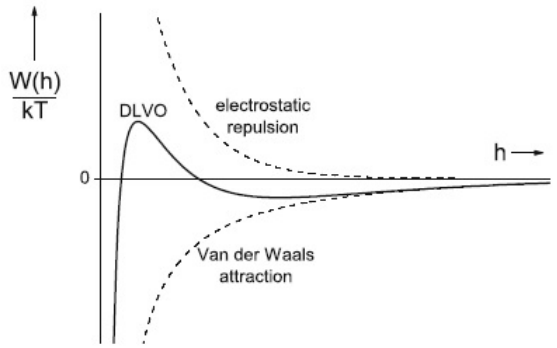

Figure 2: The Van der Waals, Double Layer and DLVO potential plotted as a function of h, the closest distance between the surfaces of two spherical colloids.[12]

Inserting the formulas for the Van der Waals (equation 2) and the double layer potential (equation 9) we get:

$$W_{DLVO} = -\frac{A}{6}\frac{2R^2}{h^2+4Rh} - \frac{2R^2}{h^2+4Rh+R^2} - \ln\left(\frac{h^2+4Rh}{h^2+4Rh+R^2}\right) + \pi\,\epsilon_0\,\epsilon\,a\,\psi_0^2\,\frac{\mathrm{Exp}[\kappa(a-r]}{r/a} \tag{11}$$

There are two special cases of the DLVO potential, one is the case of index matched particles and one is the case of a high salt concentration. In the case of index matched particles the Hamaker constant becomes zero. This results in DLVO potential which consists of only the double layer repulsion. In the case of a high salt concentration the Debye screening length gets very small, see equation 5. This will result in a small value for the double layer potential and thus a small double layer. It is important to find a good balance for the salt concentration, on one side you do not want the particles to aggregate while on the other side you want the double layer to maintain a rod-like shape. You want to maintain this shape in order to study the behaviour of rod-like particles instead of spheres. This balance can be found by adding a specific amount of salt to the solvent.

Our system consists of rod-like particles instead of spheres. This results in different potentials. In the *Mathematica* notebook, see appendix A, you can find the calculations for the Van der Waals, Double layer and DLVO potential in the case of rod like particles. The potentials are shown in figure 3.

2.2.4 Depletion interaction

When small particles are added to the colloidal suspension the behaviour of the colloids will change. These small particles called the depletant can be either hard spheres or small polymers, as long as they are non adsorbing particles.In both cases the depletant will be treated with the hard sphere potential.

There are two ways to explain the depletion interaction. One way is by the entropy gain of the depletant, the other by the osmotic pressure exerted on the colloids. The entropy of the depletant is defined by the volume in which they can move. The depletant will move in the free volume

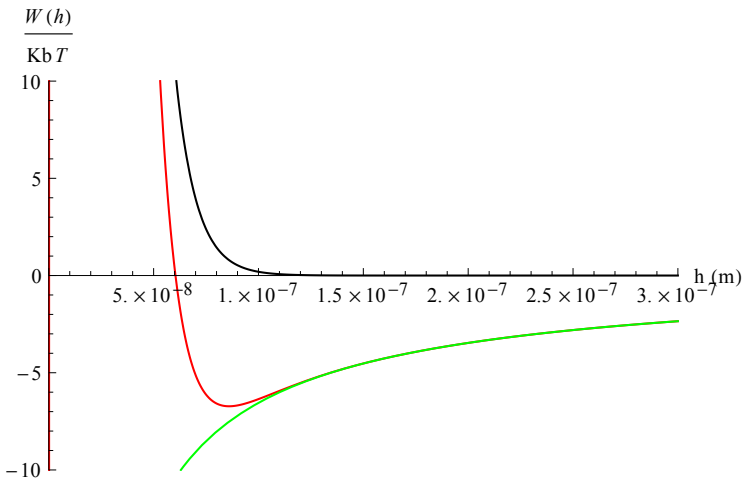

Figure 3: The DLVO potential is given by the red line, the Double Layer potential by the black line and the Van der Waals potential by the green line. h is the distance between the surfaces of the rod.

$V_f = V - N \cdot V_{coll}$ where V is the total volume, N the number and V_{coll} the volume of "big" colloids. It is possible to imagine a radius (R_d) given by the summed radii of the colloid and the depletant, see figure 7. If two colloids get close to each other the bigger spheres with radii R_d will start to overlap and create an overlap volume. Due to this overlap volume the remaining free volume for the depletant will increase and thus its entropy. Another explanation is that due to Brownian motion the depletant constantly "bumps" into the colloids. The fact that the depletant cannot be in the region between the larger colloids when their overlap volumes start to overlap will result in a net force driving the colloids together. This net force is caused by the unbalanced collisions of the smaller depletant. This net force can be directed towards either a wall or another particle. In this last case it will make the colloids attractive. (see figure 4)

The depletion interaction depends on the overlap volume between two neighbouring particles and the depletant number density, the bigger the number density the greater the interaction. The overlap volume can be seen as the excluded volume of the depletant. See figure 7 for a graphic representation of the overlap volume.

The overlap volume for two spheres is given by: $V_{ov}(r) = \frac{4\pi}{3}R_d^3(1 - \frac{3r}{R_d} + \frac{1}{16}(\frac{r}{R_d})^3)$ with r the distance between the centres of the spheres, $R_d = \frac{\sigma+\xi}{2}$ the effective radius of the spheres.

As said before the depletant collides with the colloid because of Brownian motion and thus pushes the colloids closer together once there is an overlap volume. The size of this interaction is given by the overlap volume times the pressure of the depletant.

$$V(x) = \begin{cases} \infty \text{ if } r < 2\sigma \\ -PV_{ov}(r) \quad \text{if } 2\sigma \leq r \leq 2R_d \\ 0 \quad \text{if } r > R_d \end{cases} \tag{12}$$

Where the pressure P is given by $n_b K_b T$ respectively the number density of the depletant, the Boltzmann constant and the temperature. In figure 6 you can see the depletion potential for different sizes of depletant. You can see that the potential is higher for a smaller depletant but that it acts on shorter distances.

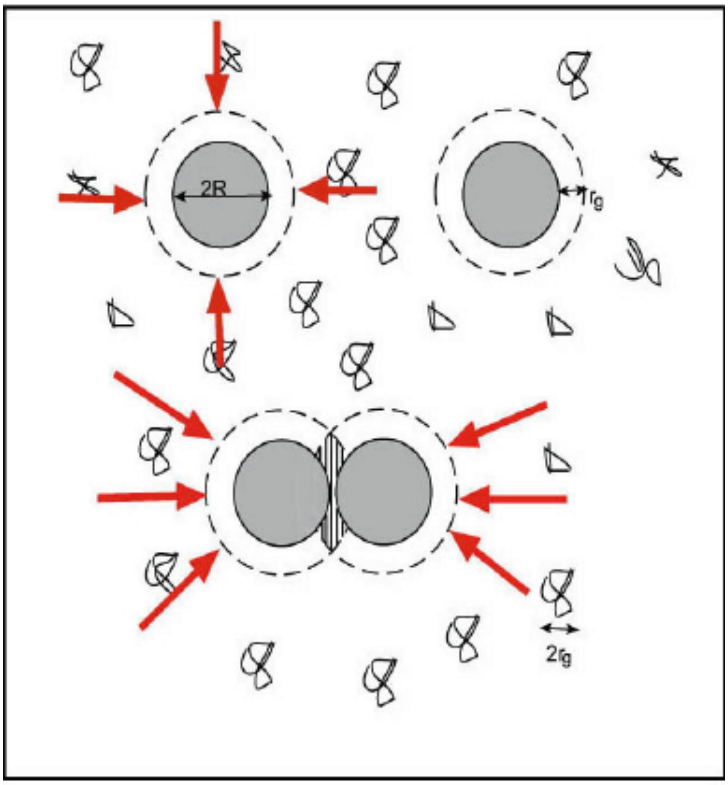

Figure 4: Two colloids surrounded by small polymers. If the colloids get close to each other the polymers will make them attractive.[19]

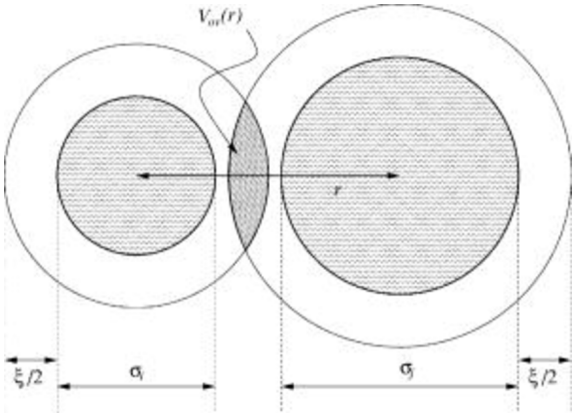

Figure 5: The overlap volume of two colloids (radius σ_i and σ_j) given by the excluded volume of depletant spheres with radius ξ [20]

The depletion interaction depends on the overlap volume of the colloids. The bigger the overlap volume the stronger the interaction. The rods can align in two different ways. They can align side to side or head to tail. The different overlap volumes are shown in figure 7. As you can see

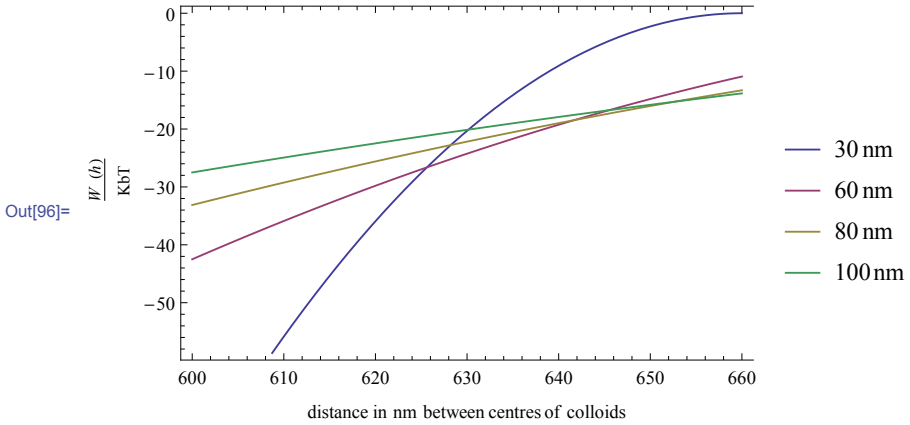

Figure 6: The depletion potential for spherical colloids with a radius of 300 nm and different sizes of depletion particles divided by K_bT in terms of the distance between the centres of colloids. Ranging from 2 times the radius of the colloid to two times the radius + 30 nm.

the overlap volume is much bigger when the rods align side to side and thus this will happen when depletant is added to the sample.

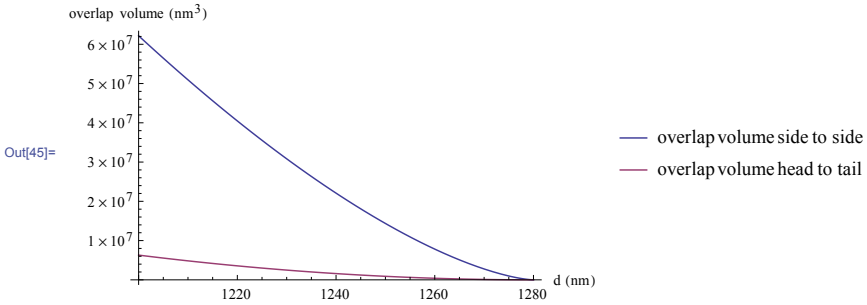

Figure 7: The different overlap volumes. d is the distance between the centres of the rods.

2.3 Liquid crystals

Almost everybody is familiar with the gas, liquid and crystal phases. The phase is determined by the amount of order in a sample. When considering anisotropic particles it is possible to find extra phases. For rod-like particles these phases are called the nematic, smectic and columnar phase. Together these are called the liquid crystals. In a crystal there is directional order and positional order in three dimensions, in a liquid crystal however there is positional order in only one or two dimensions, see figure 8

The gas and phase only differ in density, in all three cases there is neither positional nor orientational order. In the nematic phase there is only orientational ordering. There exist various types of smectic phases which differ in the amount of order. Just as in the nematic phase there is orientational order but in a smectic phases there is also positional order. This positional order is in one and/or two dimensions. The smectic-B phase for example is ordered in the normal plane

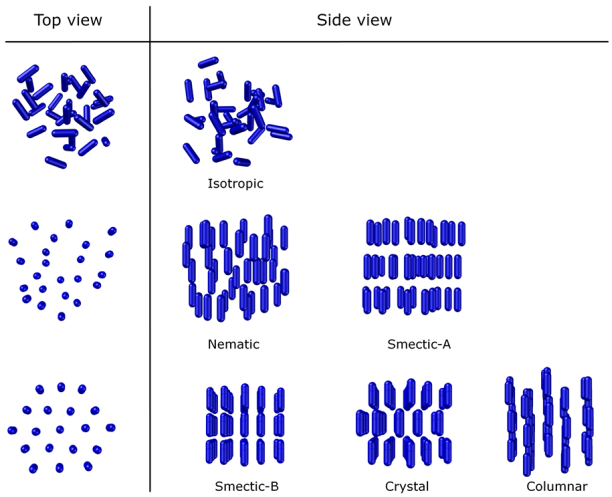

Figure 8: Graphic representation of (some of) the different phases of rod shaped particles

of the sediment. Therefore it can be seen as stacked crystalline layers. The columnar phase is orientationally ordered and positionally ordered in the z-direction. [6] See figure 8

How the rods order depends on the concentration and the aspect ratio. The aspect ratio is given by the length divided by the diameter (L/D). As can be seen in figure 9.

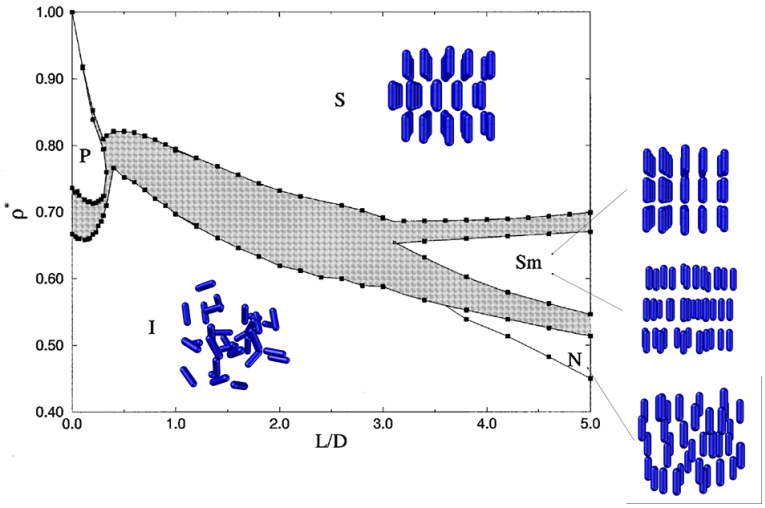

Figure 9: Phase diagram for a system of rod-like particles. The aspect ratio is plotted against the density of the species. I indicates the isotropic phase, N the nematic, Sm the smectic and S the crystal phase. The grey areas indicate coexistence.

2.4 Order parameters

To express the amount of order in a sample order parameters are defined. If the outcome of the order parameter is zero, there is no order. If the outcome is non-zero there is some kind of order. It is possible to normalise the order parameter in which case fully ordered means the order parameter is one. Below the nematic and smectic order parameters will be explained. The columnar order parameter will not be treated because our rods do not align that way.

2.4.1 Nematic order parameter

The nematic phase has a higher order than the isotropic phase. The particles are orientationally ordered. To define the nematic order parameter we first have to look at the properties. First the parameter has to be zero when the particles are not aligned and non-zero when there is some alignment. For this we use the dot product between the orientation of the particles ($\mathbf{p_i}$) and the normal direction ($\mathbf{n}$). But since the $-\mathbf{p_i} = \mathbf{p_i}$ we have to take the square. [2] So we would get the nematic order parameter: $S_i = \frac{1}{4\pi}\int_0^{2\pi} d\phi \int_0^{\pi} cos^2(\theta)\, d\theta$ which equals 1/3 instead of zero. To compensate for this we substract 1/3 of the function for S resulting in the correct nematic order parameter. After we normalise the function, meaning $m = 1$ corresponds to maximal ordering we get the following function for S [6]:

$$S = \frac{1}{N}\sum_i \frac{1}{2}(3\,\cos^2(\vartheta) - 1) \tag{13}$$

2.4.2 Smectic order parameter

In a smectic phase there is not only orientational order but also translational order. Thus the order parameter must also depend on the positions of the particles. The smectic order parameter is given by:

$$\tau = \max_d \left| \sum_{j=1}^{N} e^{i2\pi \mathbf{r_j}\cdot\mathbf{n}/d} \right| \tag{14}$$

Where d is the layer spacing for which you must take the maximum value, $\mathbf{r_j}$ the position of a particle and $\mathbf{n}$ the nematic director. [21] For confocal data the error in τ is too big, thus we must define another, more local, order parameter. We define the following order parameter: $\tau_i \equiv S_i\Delta_i$ where m_i is the nematic order parameter and Δ_i gives a measure of the distance between the centres of mass of the particles.

$$\tau_i \equiv S_i\Delta_i = S_i \cdot \left(1 - \frac{1}{m_i}\sum_{j=1}^{m_i} \frac{\mathbf{r_{ij}}\cdot\mathbf{n}}{(L_i + D_i)/2}\right) \tag{15}$$

where m_i is the number of neighbours, $\mathbf{r_{ij}}$ the distance between the centres of mass, $\mathbf{n}$ the nematic director, L_i the length and D_i the diameter of a rod. [22]

[2] $(\mathbf{p_i}\cdot\mathbf{n})^2 = cos^2(\theta)$ with θ the angle between $\mathbf{p_i}$ and $\mathbf{n}$.

2.5 Sedimentation

To locally increase the density of the rods we let them sediment. The sedimentation of the rods will result in a density gradient along the z-axis of the sample. Because the density of the rods is higher than that of the solvent the rods will sediment. This will result in higher volume fraction of rods at the bottom of the sediment than at the top which will result in a sedimentation profile. Not only does the density increase, also the pressure increases. This results in an extra force pushing the particles closer together. With rods under depletion we expect to find (from bottom to top) and depending on the aspect ratio of the rods a crystal, smectic, nematic and isotropic phase, see figure 9. The volume percentage of depletant necessary to reach the same ordering as in a monolayer is less than the % (v/v) needed for the monolayer. When no depletion is being used we expect to find a crystal, a nematic and an isotropic phase. Depending on the aspect ratio (L/D) of the rods we expect to also find a smectic phase between the crystal and nematic phase.

Why do we not always find a crystal in a system with depletant? In order to form a crystal the system needs to settle slowly. When the depletion potential is higher than the thermodynamic energy of the colloids, the colloids will be "glued" together. These clusters will sink to the bottom and it will be almost impossible for rods to "escape" the cluster. Because of this, two clusters of rods with their nematic director pointing in a different direction will not be able to align. And thus a crystal will not be formed.

2.6 Imaging

Another good reason for studying colloids is that it is fairly easy to image them. It is possible to incorporate a fluorescent label around the colloids or to even make them entirely fluorescent. This fluorescence is used when imaging the colloids with a microscope. A laser beam of a particular wavelength is sent towards the sample. The fluorescent particles emit light of another wavelength which is detected by the microscope. In order to image the sediments we use *Confocal Laser Scanning Microscopy* also referred to as confocal microscopy. Advantages of the confocal microscope in comparison to other microscopes are the point by point illumination of the sample and the rejection of out of focus light. Laser light (the blue line) is directed towards the sample by a dichroic mirror. (Light of certain wavelengths passes through a dichroic mirror while other wavelengths are reflected.) The confocal microscope scans through the sample using two rotating mirrors that focus the light of the laser on a specific part of the sample. The fluorescent sample emits light of a different wavelength (the green line) which is redirected by the rotating mirrors, passes through the dichroic mirror and through the pinhole. This pinhole rejects out of focus light, emitted by particles which are not in the focal plane, thus reducing the blur of the image. [23]

The resolution of the microscope depends on the diffraction of light. It is impossible to see images smaller than the wavelength of the light being used. The image of a perfectly focused point trough a circular aperture is known as the airy disk. The size of the Airy disk depends on the wavelength of the laser beam and the numerical aperture of the objective lens.[23] [24] The numerical aperture (NA) is given by: [25]

$$NA = n \sin(\vartheta) \tag{16}$$

Where n is the refractive index and θ the semi-angle of the light cone refracted by the sample. The NA gives a measure of the light-gathering power of the objective and of the highest achievable

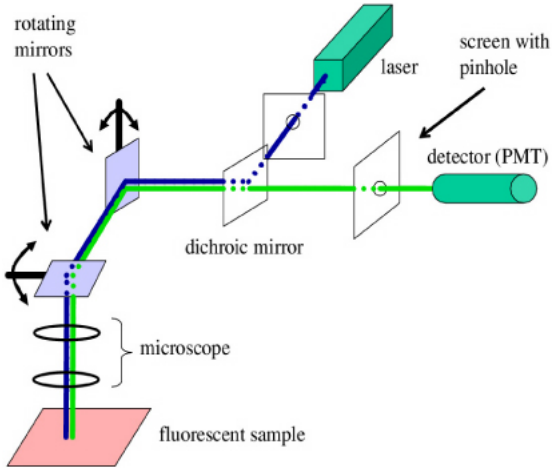

Figure 10: A schematic image of a confocal microscope. Laser light is emitted by the laser, gets reflected by the dichroic mirror and is than pointed at the sample using rotating mirrors. The fluorescent sample emits light of a different wavelength which the mirrors reflect back towards the dichroic mirror which lets this wavelength through. The light beam goes through the pinhole and into the detector creating an image.

clarity. The greatest NA is achieved with an oil immersion lens and is 1.4. [26] This gives a resolution of around 200 nm. The 3D analogy of the Airy disk is the Point Spread Function (PSF). The PSF gives a measure for the resolution in the x, y and z direction. By calculating the PSF of the microscope and applying this to the images it is possible to increase the resolution. Fluorescence microscopy gives two types of blurring. One is given by the noise and the other one by the PSF of the microscope. The noise can be reduced by the use of a pinhole (optical deconvolution) as is done by a confocal microscope and correction for the system's PSF can be done by computational deconvolution.

3 Experimental

3.1 Synthesis

In order to be able to do the experiments we need both rods and depletant. The syntheses done are described below.

3.1.1 Rod synthesis

The synthesis of a batch of rods consists of three steps. First you grow the core of the rods. Around the core you grow one fluorescent shell around which you can than grow multiple non-fluorescent shells, see figure 11. With the amount of non-fluorescent shells you can control the size and aspect ratio of the rods. The rods were synthesised following a procedure described by A. Kuijk. [27]

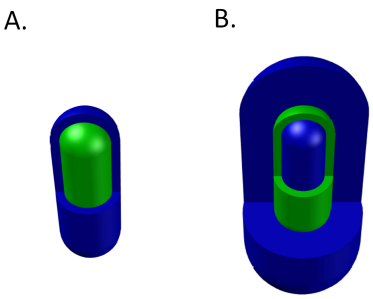

Figure 11: In A. you see the rod with a fluorescent shell (green) and one non fluorescent shell (blue). In B. you see the rod (blue) with one fluorescent and multiple non fluorescent shells. The multiple non fluorescent shells are needed to distinguish the particles from one another.

We start with the cores, these will be grown in a water in oil emulsion. The rod will emerge from the water droplet as the precursor tetraethylorthosilicate is added to the emulsion. The precursor requires water for the hydrolysis reaction and therefore can only take place in the water droplet. This results in the one sided addition of material thus creating a particle with a rod-like shape (as shown in figure 12). There is also some ammonia present, which acts as a catalyst for the hydrolysis and condensation reaction, in the mixture. By varying the ammonia concentration the length of the rods can be tuned. For the rods to be visible under the confocal microscope they must be fluorescently labelled. This will be done by growing a fluorescent shell around the rods, the dye used to achieve this fluorescence is FITC (Fluorescein isoth- iocyanate) which is exited at a wavelength of 495 nm and emits a green light at 519 nm. [28] Instead of growing a fluorescent shell around the rods it is also possible to fluorescently label the cores themselves. But because this results in a gradient in the intensity along the length of the rod we chose for a fluorescent shell. Around this fluorescent shell multiple non-fluorescent shells must be grown in order to distinguish the particles under the confocal microscope.

The synthesis of the cores will be done in a PVP/1-pentanol solution which is made by adding 80 grams of PVP (wt 40 000 Sigma Aldrich) to 800 ml 1-pentanol ($\geq$ 99 % Honeywell) in a 1 litre flask. It is important that the PVP is completely dissolved. In order to achieve this one must

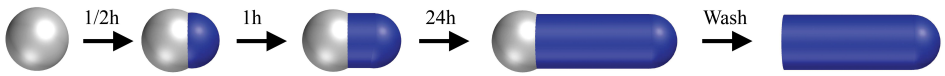

Figure 12: The silica rod (dark blue) grows from a water droplet (silver).

shake the mixture. If not completely dissolved let the mixture rest 2 days in order to achieve this. To grow the rods add 80 mL of ethanol (100 % Interchema), 22 mL of Milli-Q ultra pure water and 5.33 mL sodium citrate dehydrate ($\geq$ 99% Sigma Aldrich) as quick as possible to the 1 litre flask with PVP/1-pentanol. Than add 17.7 mL ammonia (25.5 % Honeywell/Fluka) and quickly add 6.67 ml of Tetraethyl orthosilicate: TEOS(98 % Aldrich). Shake the flask immediately and let it rest for two more days. Wash the rods by replacing the PVP/1-pentanol solution once with ethanol, once with water and finally two more times with ethanol.

To increase the monodispersity of the rods one can get rid of the bigger particles and the smaller particles. In order to remove the bigger particles one must centrifuge at a low speed (40 g for 20 minutes), take the supernatant and store this in another bottle. Add more ethanol, sonicate the flask and repeat this process twelve times. All the good particles can now be found in the supernatant you segregated. In order to remove the smallest particles one must centrifuge at such a speed that a sediment can be seen at the bottom of the vial (7000 g for 15 minutes). Now you remove the supernatant which contains the smaller particles, add more ethanol, sonicate and repeat this procedure fourteen times. To make these techniques more efficient one must divide the rods over multiple vials.

To grow a shell around 100 mgr of rods, put the rods and 80 mL ethanol (100 % Interchema) in a round bottom flask, add a stir bar and put it on a magnetic stirrer. Add 5 mL Milli-Q ultra pure water, 6 ml of ammonia (25.5% Honeywell/Fluka) and 1 ml of APTES(3-Aminopropyl triethoxysilane)-FITC (Fluorescein isoth- iocyanate) mixture [3] and cover the flask in aluminium foil. Stir the mixture well and add 20 μL of TEOS (98% Aldrich) six times 15 minutes apart, let the mixture rest for two hours after adding the last injection of TEOS. Wash in ethanol four times. To do this, centrifuge 20 minutes at 7000 g, remove the solvent, add ethanol, sonicate until the rods are dissolved and repeat this procedure several times.

The procedure for growing non-fluorescent shells is the same as for the fluorescent shell, only the dye mixture must not be added and 20 μL of TEOS (98% Aldrich) (per 100 grams of rods) must be added a total of 8 times instead of 6 times. Note that it is important to determine the amount of rods you start with for every additional shell you are growing. To remove secondary nucleation and aggregates of rods the batch must be washed again using the method described above to increase the monodispersity.

3.1.2 Depletant synthesis

The silica spheres of which the depletant consists were made using a Stöber reaction as described by W. Stöber. [29] Put 500 mL ethanol (100 % Interchema), 33.3 mL ammonia (25.5 %, Honeywell/Fluka) and a stir bar in a 1 L round-bottom flask and put it on a magnetic stirring plate, creating a big vortex. Add 20 mL TEOS (98 %, Aldrich) all at once and let it stir overnight.

[3] For 100 mgr of rods one needs a mixture of 5 mgr of FITC($\geq$ 90.0 % Sigma Aldrich) dissolved in 1 ml of absolute ethanol, add 7 μL of APTES (99 % Sigma Aldrich) and let it stir overnight in order to couple the FITC to the APTES.

Wash the particles in ethanol multiple times by centrifuging 20 minutes at 15000 g, removing the solvent, adding ethanol, sonicating until the rods are dissolved and repeating this procedure various times. The monodispersity can be increased using the same method as used for the rods.

3.2 Imaging

In order to study the self assembly of rods under depletion we must be able to image them. The imaging of the rods consists of various steps. First a sample must be made, second you look at the sample using a confocal microscope, next you deconvolve the image and lastly you track the rods using the rod tracking code. These steps will be explained in more detail in the following paragraph.

3.2.1 Making the sample

A microscopy cell must be made using a microscope slide with a circular hole with a diameter of 7mm, a cover slip and a glass Pasteur pipette. The length of the end of the paseur pipette is 25 mm, the outside diameter is 6.75 mm and the inside diameter is 5.2 mm. Cut off the end of the pipette using a diamond glass cutter, glue the cover slip under the microscope slide covering the hole using UV-glue (Nordic 68) and mount the pipette top on top of the microscope slide. Glue this all together and let it harden under the UV lamp. To seal the cell make small ball of surgical cotton wool and parafilm ("M"). After adding the rods and depletant to the cell one closes it completely using candle wax.

3.2.2 Acquiring the images

To get a high quality image of the system it is important that the rods (and spheres) are index matched with the medium. The refractive index of the rods can be measured using a Atago refractometer. Note that because we index match the rods this also results in a Van der Waals potential equal to zero.

All confocal microscopy images were taken using a Leica TCS SP8 equipped with a CW depletion laser and a 100×/1.4 confocal oil immersion objective at a wavelength of 488 nm by using a solid state laser. The following configurations were used: Multiphoton Laser off, Sted3D on and resonant mode on. Resonant mode must be used because it allows quick scanning which is needed in case the particles move to fast. The format of images taken was 512x512 with a scanning speed of 12000. The pixel size was 50 by 50 nm and the sample was scanned in the bidirectional mode. The pictures cannot be much larger because in order to track the rods their diameter (in every direction) must be at least five pixels. The complete settings can be found in appendix B We have made both images at different heights as well as z-stacks of the entire sample. The pictures to give an idea of what we are dealing with and the z-stacks in order to analyse the data. When making a z-stack it is important to start scanning at the top of your sample because of the intensity of the particles. When starting at the bottom it is possible that the top particles will have lost their fluorescence and therefore will not be visible anymore. After making the z-stack the *Huygens Professional* deconvolution software is used to increase the image. This software reduces the blur and calculates the microscopes PSF using the microscope settings.

3.2.3 Rod tracking

To make an animated 3D representation of the sample the rods need to be tracked. This is done using the rod-tracking code written by T. Besseling et al. The code applies several steps to the confocal image in order to obtain the final image. First a Gaussian filter is applied to reduce the background noise. Next it finds the locations of the particles by selecting pixels with a specific intensity and scanning around these pixels within a radius of 2 pixels in order to see which pixels belong to the same particle. Next it compares the orientation of the particle with the x-axes. Then it draws a line through the pixels of one rod and rods can be removed if their intensity is too low or when they are too small. [7]

3.3 Analysis

The coordinates given by the rod tracking code are used to analyse the samples. This data consists of the locations and directions of the rods. A density plot was made looking at the amount of particles at different heights. This shows the density at various heights in the sample. Next, the nematic order parameter was calculated using equation 13. A difference has been made between the overall nematic order parameter, which compares the angles of individual rods to the average (taken over all rods) nematic director, and the local nematic order parameter, which compares the angles of individual rods to the angle of the rods surrounding this rod. In this last case you look at the amount of order of a rod in comparison to the rods surrounding it. This last calculation gives a better idea of the order of the system since the depletant gives rise to ordered clusters and not overall ordering. Last the smectic order parameter was calculated using equation 15. For S_i we chose the local nematic order parameter since this gives a better indication of our system. The calculations can be found in the appendix A. To determine whether a system is in an isotropic (I), nematic (N) or smectic (S) phase we used the following thresholds as defined by H. Bakker [30]:

$$\begin{aligned} I &: \langle S_i \rangle < 0.5 \text{ and } \langle \tau_i \rangle < 0.35 \\ N &: \langle S_i \rangle > 0.5 \text{ and } \langle \tau_i \rangle < 0.35 \\ S &: \langle S_i \rangle > 0.5 \text{ and } \langle \tau_i \rangle > 0.35 \end{aligned} \tag{17}$$

4 Results and Discussion

4.1 Rod and depletant synthesis

The batches of fluorescent silica rods and silica spheres were produced using the methods described above unless mentioned otherwise. The cores produced (DD01) are 2189 nm long with a diameter of 315 nm resulting in an aspect ratio [4] of 6.9. After thorough washing the polydispersity of these particles was reduced to 8.9 %. The cores used to grow (non-)fluorescent shells around were synthesised by A. Grau Carbonell. Two batches of rods were created from these cores and these are the rods used for the experiments. Both batches have one fluorescent shell. AGF1NF4 has four non-fluorescent layers and AGF1NF2 has two non fluorescent layers. More layers makes it easier to distinguish the rods but at the same time lowers the aspect ratio and increases the weight thus decreasing the gravitational length of the particles. The spheres DD01 have been produced by the method described above but particles with a higher monodispersity (RD290) have been synthesised by R. Moes as described by S. Shabibi et al. [31] and W. Stöber et al. [32] All rods and spheres used are listed in table 2. In figure 13 the TEM-images of AGF1NF4, DD01 and RD290 are visible. Notice the visible difference in aspect ratio between the coated and non-coated rods. Images of the other particles are not given but resemble the particles shown here.

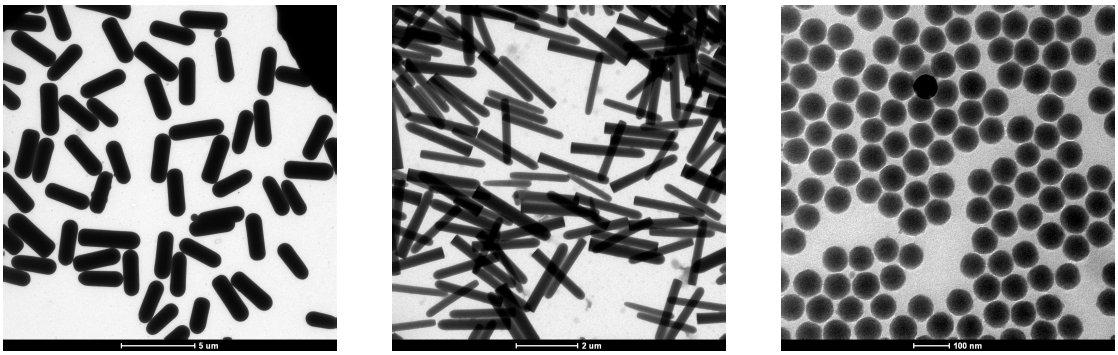

Figure 13: From left to right, TEM images of AGF1NF4, DD01 and RD290.

Name	diameter (nm)	length (nm)	Aspect ratio	polydispersity (%)
AGF1NF4	1080	3247	3.0	9.3
AGF1NF2	623	2653	4.3	11.9
DD01	315	2189	6.9	8.9
DDSph01	43		1	13
RD290	35		1	3

Table 2: The name, size and polydispersity of the batches of rods and spheres used.

[4] Aspect ratio = Length/diameter

4.2 Influence of the depletant in monolayers

Adding depletant to the sample results in an attractive potential of the rods. The strength of this attractive potential is governed by the amount of depletant added and the size of these spheres. All the experiments were done using 80 nm spheres and thus the volume percentage of depletant was varied to change the strength of the attraction. At a concentration of 3.75 % (v/v), see figure 14.A, the sample shows no positional or orientational order, small clusters of 3 to 5 particles are visible but there is no long range order. The picture shows an isotropic phase. In figure 14.B a monolayer with a depletant strength of 6.75 % (v/v) is shown. Long rows are clearly visible and some ordering between different rows can also be seen. Picture B shows long rows of particles which are pointing in the same direction, some of these rows are ordered with respect to each other. This is called a smectic phase. In figure 14.C a monolayer with a depletion strength of 13.5% (v/v) is shown. The clusters vary in length ranging form approximately 3 to 16 particles. Also visible are particles standing upright, which we did not see in samples with a lower depletion strength. In this sample there are some rows but they are shorter than in sample B but here is also some ordering between different rows visible. You can clearly see that of these three samples, sample B has the highest amount of order. So there is an optimum of depletion strength somewhere between 3.375 and 13.5 % (v/v). The order first increases but after a certain amount of depletant has been added the order starts to decrease.

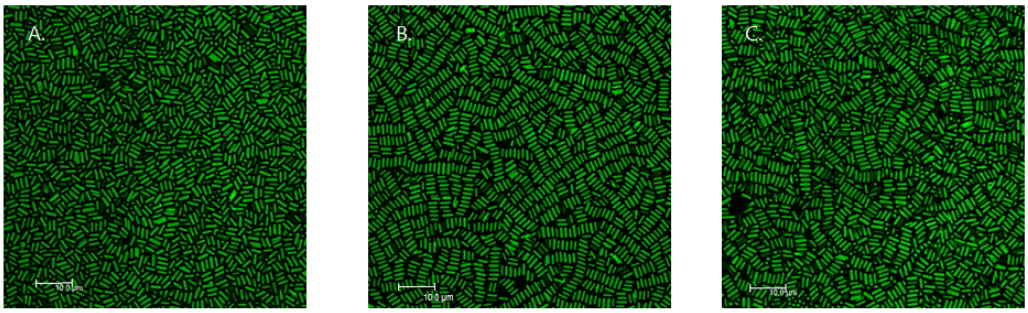

Figure 14: A monolayer of AGF1NF4 with different volume percentages of depletion. From left to right: 3.375 % (v/v), 6.75 % (v/v) and 13.5 % (v/v). You can see that the highest order is achieved for 6.75 % (v/v). All scale bars indicate 10 µm.

4.3 Influence of the depletant in sediments

As said before, in sediments there is a density gradient along the z-axis. The density of and the pressure on the rods is higher at the bottom of the sediment than at the top. Multiple samples with varying % (v/v) of depletant and rods have been made using the techniques described in section 3.2.1. The samples have been studied both after one day and after three weeks. In the absence of depletion there is very little ordering of the AGF1NF2 rods after one day. No rows of particles have been formed. The system consists of a large isotropic phase and a small nematic phase, no smectic phase can be found. A sample of the bigger rods (AGF1NF4) shows great order after three weeks, a crystal is clearly visible followed by a small isotropic phase. To reach

a crystal a certain pressure upon the particles is needed, in the case of this sample the pressure exerted on the particles is large enough because these rods are very heavy. This does mean though that it is not a good comparison with the other samples since these are made with the smaller, lighter rods.

The sample with 0.5 % (v/v) depletion (GD2) shows some order at the bottom after one day. There are some rows of of aligned rods and some of these are nicely aligned with a neighbouring row. Above this bottom layer there are a couple of layers with very little ordering. But at 1/3 of the sample you see a smectic phase begin and halfway the sample an isotropic phase starts. In short you see a very large isotropic phase on top of a small smectic phase on top of a dense but isotropic phase. Interesting is that there is little order at the bottom in comparison with higher in the sample. This is unexpected. It might be explained by the fact that the particles on the bottom have so much pressure on them that they are "frozen" in the clusters they formed and the beginning and need more time to settle. This while the particles higher in the sample have less pressure exerted on them and are thus freer to move. The rods try to achieve the highest possible order, to do this they must be able to settle. In other words they must be able to escape from the depletant interaction and align with other particles. When the pressure exerted on the particles is to big the system can not settle. If the pressure is high but not too high the system will need more time to settle than just one day. Snapshots of the bottom, the smectic phase and the isotropic top phase can be seen in figure 15. When looking at the same sample after three weeks (GW2) the bottom is still not ordered but the smectic phase begins lower in the sample. Also noticeable is that after three weeks the isotropic phase at the top of the sample has become much smaller.

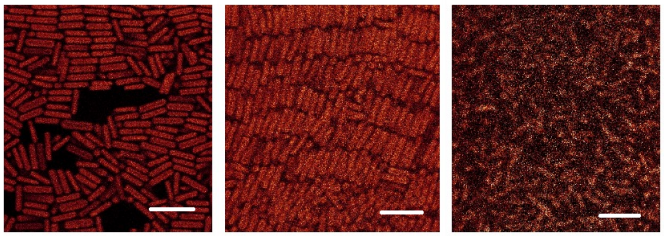

Figure 15: From left to right, the bottom layer, a smectic layer halfway through and the top layer of sample GD2 with 0.5 % (v/v) of depletion. All scale bars indicate 5 µm

Sample GD3, with 1.0 % (v/v) of depletant is similar to GD2 but the bottom layer has more order. The clusters seen here are a little bit longer. But in the layers above little order can be found, until again at approximately 1/3 of the sample where a smect begins. Which at 3/4 of the sample turns into an isotropic phase. GW3 (GD3 after three weeks) is an interesting sample. There are some gaps between the particles as you can also see in figure 15 at the bottom of the sample with 0.5 % (v/v). The smectic phase has decreased in size and it looks like the isotropic phase has increased in size. This is probably not correct and the sample may been shaken too much.

Sample GD4, with 2.0 % (v/v) of depletion, exhibits almost the same behaviour as GD2 and GD3 except that the bottom layer is quite ordered. Above this bottom layer there are some disordered layers. Again at around 1/3 of the sample a smectic phase starts and halfway through the sample a large isotropic phase begins. Three weeks later the sample looks less ordered, the bottom layer is not ordered anymore and neither are the layers above. There are two possible explanations,

one is that the sample has moved to much and has thus lost it's order. Another, more likely, explanation is that the DMSO has reacted with the glue making the sample leak particles. Higher in the sample a small smectic phase is still visible. This smectic phase is followed by a isotropic phase.

The sample with 5 % (v/v) depletant is a very dense sample. The bottom layer is quite ordered, there is in some cases also ordering between different rows of rods and in some cases the second layer is orderly stacked upon the bottom layer. This is however not the case for all clusters. The bottom layer is better ordered than the layers following but in every layer there rows of rods can be found. There are some gaps visible in the sample and there is no isotropic phase. Three weeks later the sample still looks (almost) the same. There are still some big clusters of particles but the sample is not entirely ordered.

The last sample with 7.5 % (v/v) depletant is locally ordered along the whole sample. There are no single particles. All particles are connected to a row. Again there is no isotropic phase and the sample has barely changed over three weeks. This probably means that the depletion interaction is too strong for the sample to settle. The rods cannot escape from a cluster to align with another (larger) cluster. For these samples to settle will take a very long time. Noticeable is that the sample seams smaller than before, this might also be explained by loosing particles due to the interaction of the DMSO with the glue.

From what we discussed above you can conclude that samples with a high depletion volume percentage show more order on short timescales but less order on longer timescales. This might be because the depletion interaction is stronger than the thermal energy of the rods, another possible explanation is that the glue might be leaking. Therefore they are glued to their cluster. In all cases the isotropic phase shrunk over time but not in all cases did it disappear, this only happened for high volume percentages. Noticeable was the fact that for a lot of samples the highest order was found in the middle. This was probably due to a combination of the pressure and the depletant. All the different samples are shown in table 3.

Name	**Rods**	**% (v/v)**	**Depletant % (v/v)**	**Time rested**
GD1	AGF1NF2	0.50	0.0	1 day
GW1	AGF1NF4	0.50	0.0	3 weeks
GD2	AGF1NF2	0.50	0.5	1 day
GW2	AGF1NF2	0.50	0.5	3 weeks
GD3	AGF1NF2	0.50	1.0	1 day
GW3	AGF1NF2	0.50	1.0	3 weeks
GD4	AGF1NF2	0.50	2.0	1 day
GW4	AGF1NF2	0.50	2.0	3 weeks
GD5	AGF1NF2	0.50	5.0	1 day
GW5	AGF1NF2	0.50	5.0	3 weeks
GD6	AGF1NF2	0.50	7.5	1 day
GW6	AGF1NF2	0.50	7.5	3 weeks

Table 3: Different samples made with different depletion strengths.

4.4 Tracking and analysing small sediments

Using the bigger rods (AGF1NF4) three small sediments with different volume percentages of depletant (DDSph01) have been made, one sample with 3.375 % (v/v), one with 6.75 % (v/v) and one with 13.5% (v/v). These samples have been tracked using the rod-tracking code and have been analysed using the *Mathematica* notebook.

The sample with 3.375 % (v/v) of depletant has three layers of rods. Some ordering can be seen in the bottom layer but the two layers above are isotropic. The tracking and the 3D representation from two different angles can be seen in figure 16. When looking at the sample and the z-distribution of the particles, you see that most particles can be found in the bottom layer and in every subsequent layer there are less particles. The bottom layer is clearly visible but the layers following cannot be identified as different layers. The particles are not ordered in layers. The local nematic as well as the smectic order parameter are very low for this sample. No difference can be found between the bottom and the top layer of the sediment. Using the thresholds defined before this sample is completely isotropic.

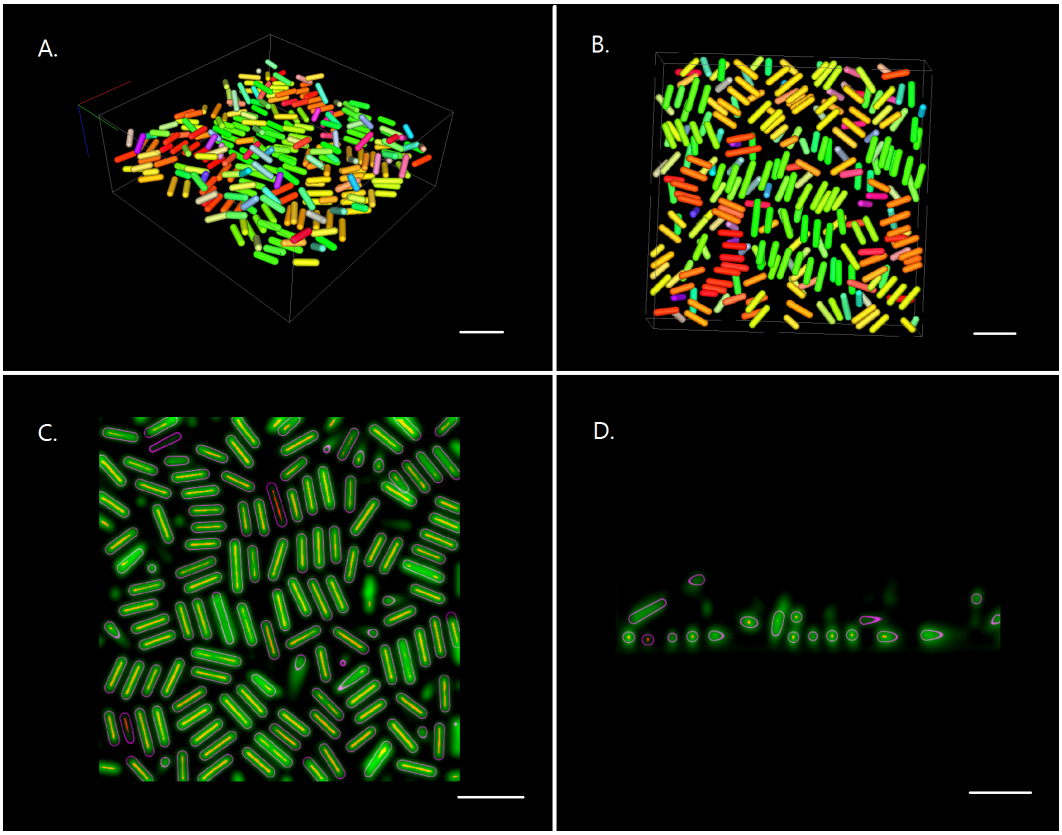

Figure 16: For the sample with 3.375 % (v/v) of depletant, A & B are the computer rendered particles, colour coded based on their orientation. A gives an overview of the sample while B shows the bottom of the sample. C & D show the top and side view of the confocal data, the identified particles are outlined in magenta. All scale bars indicate 5 µm

With 6.75 % (v/v) of depletant the sample looks quite different. The whole sample is very

ordered and the different layers are distinguishable. Long clusters of rods can be found in both the bottom and the top layer, see figure 17 A and B. The local nematic order parameter is 0.79 and the smectic order parameter is 0.78. It follows that the sample exhibits a smectic phase.

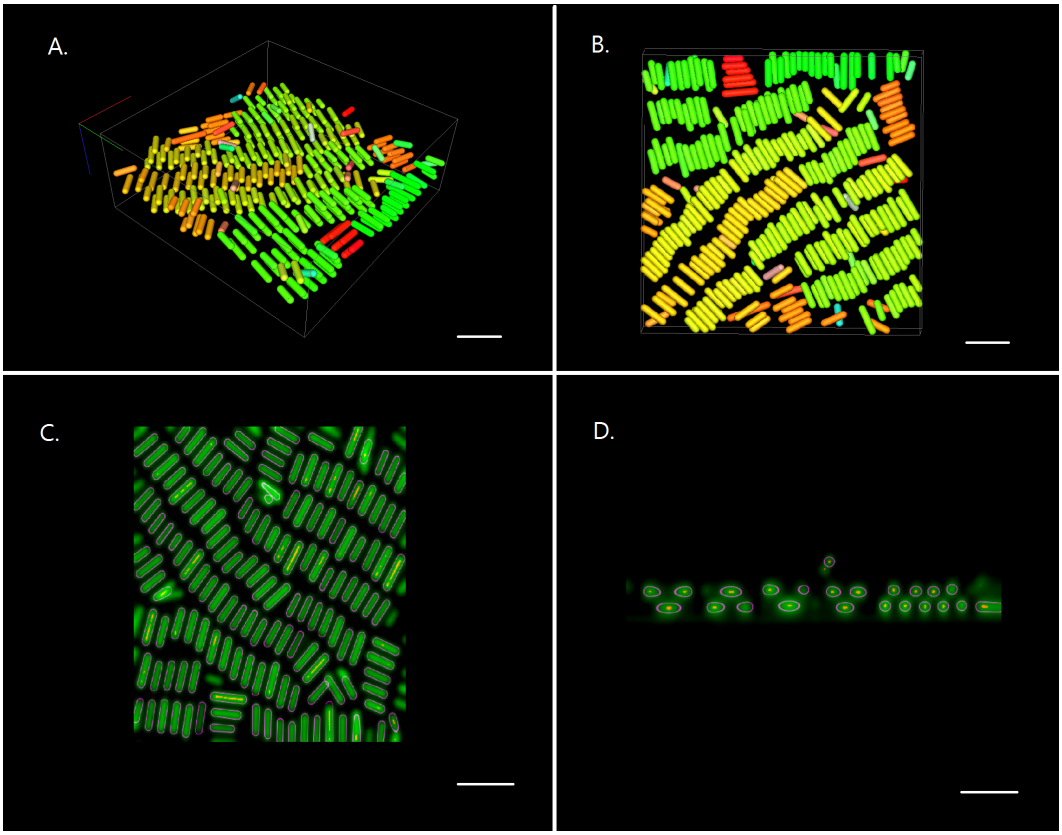

Figure 17: A (overview) & B (bottom) show the 3D image stack, C & D show the confocal data with the identified particles outlined in magenta of the sample with a volume percentage of 6.75. All scale bars indicate 5 µm

The last sample with a depletion strength of 13.5 % (v/v) differs from both samples. Looking at the 3D representation one can see clusters of ordered rods but these clusters show no mutual order, see figure 18 The highest part of the sample consist of five layers. In this sample there are also clusters of particles standing upright. We did not see this in the other samples. There are layers visible looking at the z-distribution, but you can see that particles can also be found in between these layers. There is a great difference between the global and local nematic order parameters (0.15 vs 0.53). The smectic order parameter is 0.52, so the sample is in a smectic phase, however much less ordered than the sample with 6.75 % (v/v). Noticeable is that you can see clearly that there are groups of particles anti aligned with their neighbours. This is probably the result of two neighbouring clusters with a different nematic director.

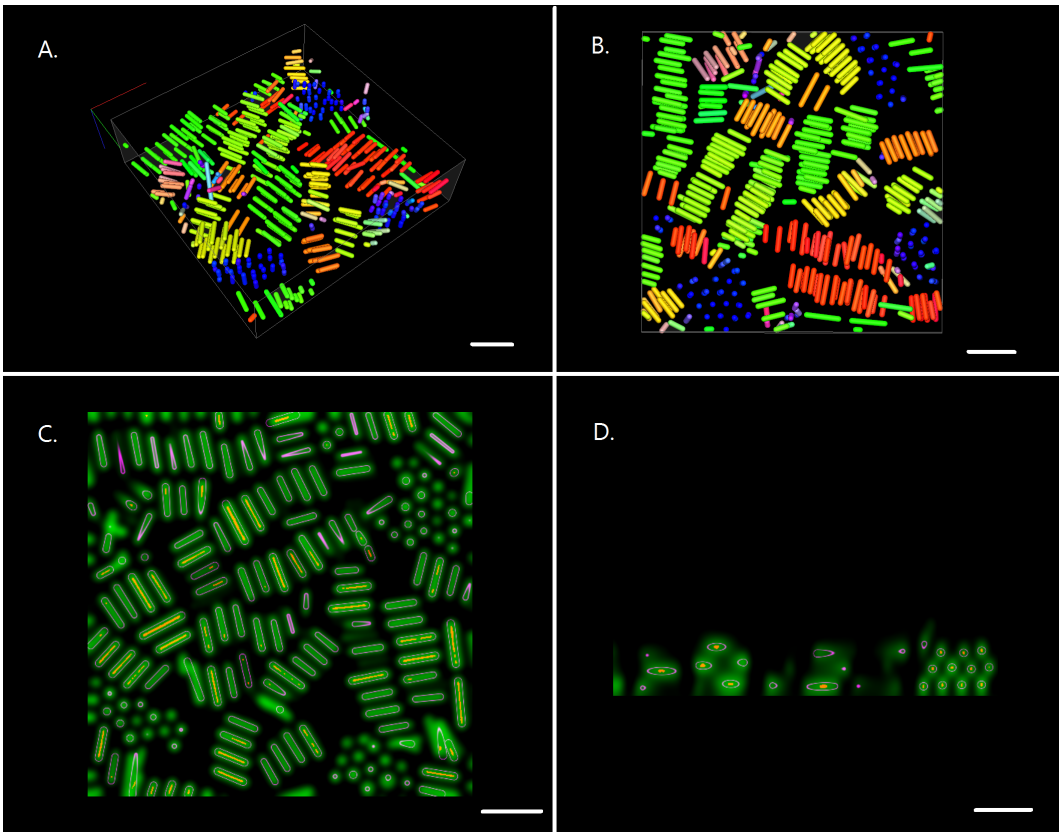

Figure 18: A (overview) & B (bottom) show the 3D image stack, C & D show the confocal data with the identified particles outlined in magenta of the sample with a volume percentage of 13.5. All scale bars indicate 5 µm

Looking at the z-distribution of the particles there is a clear bottom layer visible. With almost no depletion a second layer is visible but not all particles are ordered in these layers and after the second layer there is a gradual decrease of particles. At 6.75 % (v/v) of depletion the layers are very well defined. For the highest amount of depletant the layers can be distinguished but there are many particles in between these layers. This may partly be due to the upstanding particles which cannot be placed in a horizontally defined layer. Considering the local nematic and the smectic order parameter we notice that for the sample of 3.375 % (v/v) no order can be found, the order in the sample with 6.75 % (v/v) is very large. And as said before in the sample with 13.5 % (v/v) depletant groups of anti aligned particles and groups of nicely aligned particles can be seen.

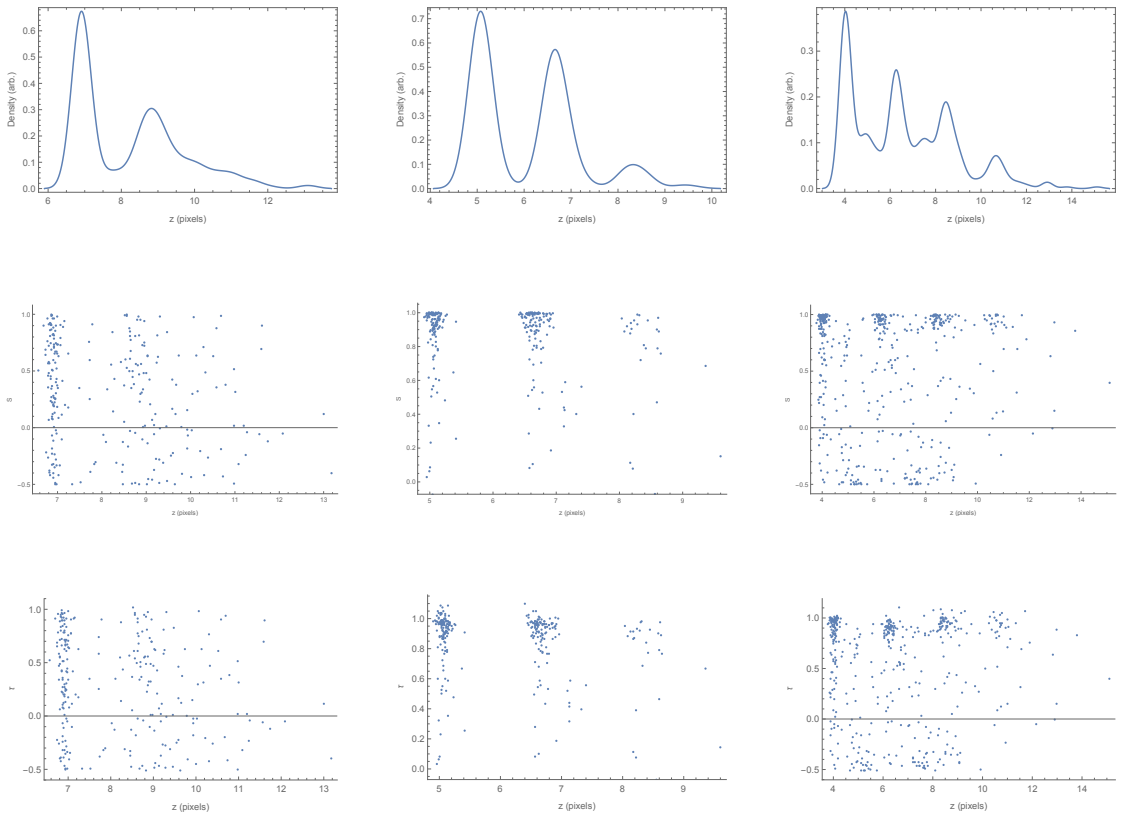

Figure 19: Above, the density of the particles plotted against z. In the middle the local nematic order parameter and at the bottom the smectic order parameter for all rows: from left to right: 3.375 % (v/v), 6.75 % (v/v) and 13.5 % (v/v).

4.5 Tracking and analysing large sediments

When considering larger sediments there are some things we should keep in mind. The pressure from above is larger, there are more particles and you do not want the depletant to sediment as well. In order to prevent the depletant for sedimenting we look at the gravitational length. We have chosen a depletant with a diameter of 80 nm, the buoyant mass of these particles is so small that they should not sediment on the timescales we are considering. The greater amount of particles will result in a larger sediment and these particles will put extra pressure on the particles below them. As for the extra pressure; rods with a high aspect ratio tend to align under sufficient pressure. The presence of a depletant will only increase this tendency to align. This means less depletant will be needed in order to form a smectic phase than when considering small sediments or even monolayers.

Different samples have been made with a depletion volume percentage ranging from 0.5 to 7.5, all using AGF1NF2 and RD290. All samples consist of 100 µL 0.14 % (v/v) of AGF1NF2 in

DMSO/H2O solution[5], 50 µL of DMSO/H20 and 150 µL of two times the final depletant volume fraction. To be able to see the difference between a sample with and without depletion, a sample with zero depletion has been made as well. In the absence of a depletant an extra 150 µL of DMSO/H20 has been added. After 1 day no order could be found. There were no clusters of particles in the sample. A sample of bigger rods (AGF1NF4) has been studied after 4 weeks, the sample was very ordered. Clear layers were visible and all particles were aligned up until a certain height, a crystal was formed. The upper part of the sample was in an isotropic state with no overall order. The explanation for this crystal has already been given in section 4.3.

The behaviour of the samples has already been described in section 4.3. The tracking of the sediments has been done the same as the small sediments but the higher you get in a sample the worse the resolution becomes because of scattering and increased movement. This makes is more difficult to track the bigger sediments. The analysis of the data has been done using the *Mathematica* Notebook. The bottom view and overview of the sediments GD2 and GW2 are shown in figure 20. The main difference between the measurements done after one day and after 3 weeks is the height of the sediment. The sediment has become more dense. When looking at the z-distribution we see the same, the sediment has become denser and shorter. The nematic order parameter has decreased a bit during the three weeks from 0.66 to 0.55. When comparing the z-distributions of the nematic order parameter nothing seems to have changed. The smectic order parameter almost has not changed, after one day it was 0.56 and after 3 weeks it was 0.54. A possible explanation in the form of the interaction between the DMSO and the glue which was mentioned above seems to be incorrect because the number of particles has slightly increased instead of decreased.

[5]The DMSO/H2O solution is made using the refractive index of the rods and matches this RI

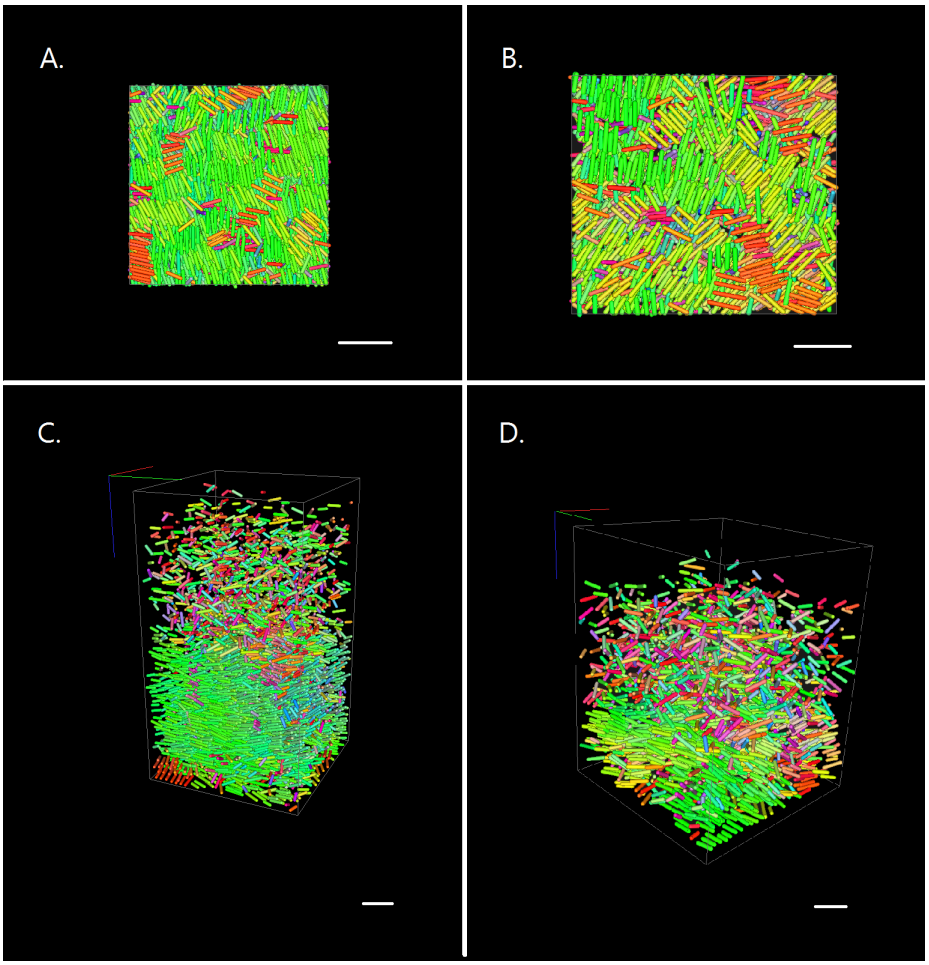

Figure 20: The computer rendered images of GD2 (A. and C.) and GW2 (B. and D.), the samples with 0.5 % (v/v) of depletant. The bottom of the sediment is shown in A. and B. and an overview of the complete z-stack is shown in C. and D. The rods are colour coded based on their orientation. All scale bars indicate 5 µm.

The density of the bottom layers of the sample with 2 % (v/v) of depletant has not increased while resting for 3 weeks, but the density at approximately 3/4 of the sample has increased. A clear drop in intensity at the top of the sediment is visible after 3 weeks. The order in the sediment has decreased strongly, large parts of the smectic phase have turned into an isotropic phase ($S < 0.5$). I have no explanation for this and it (probably) means something has probably gone wrong. It will be necessary to perform the experiment again.

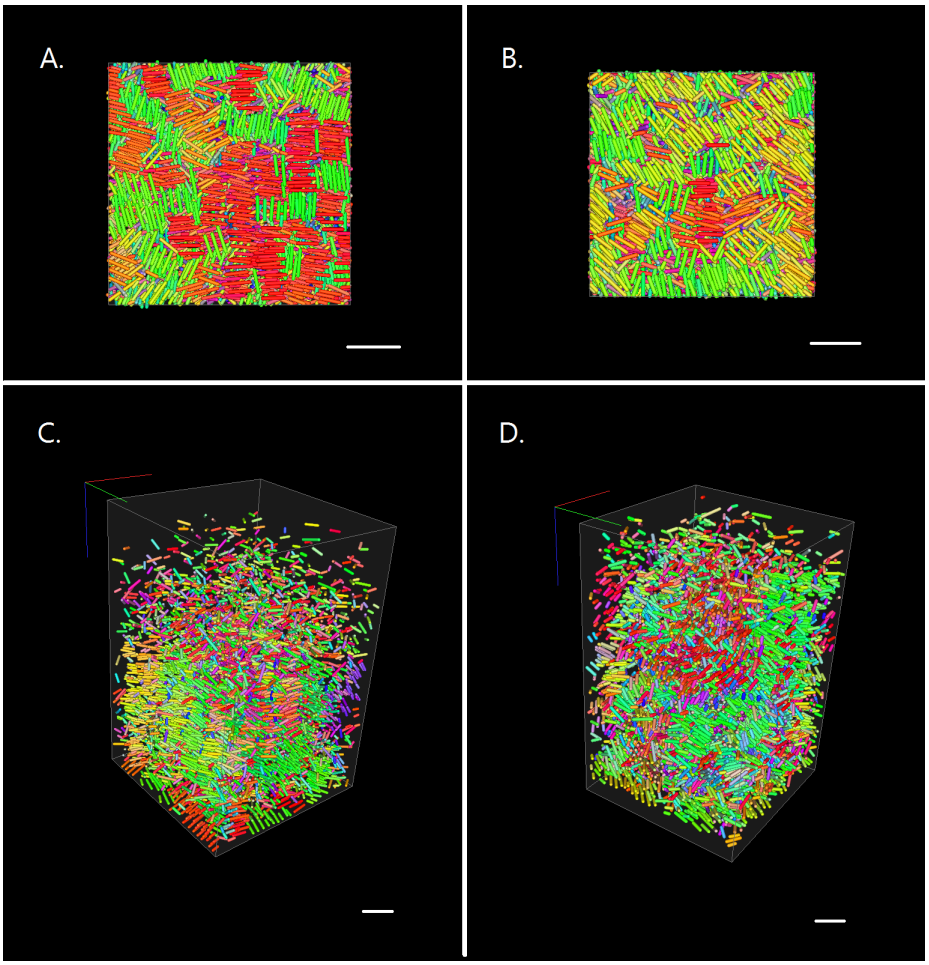

Figure 21: The computer rendered images of GD4 (A. and C.) and GW4 (B. and D.), the samples with 2 % (v/v) of depletant. The bottom of the sediment is shown in A. and B. and an overview of the complete z-stack is shown in C. and D. The rods are colour coded based on their orientation. All scale bars indicate 5 µm.

At a high concentration of depletant such as 5 % (v/v). The rods align in long rows already after one day. The sample is more compact after resting for three weeks. And when looking at the images (see figure 22) you would say that the isotropic phase is completely gone. But when considering the thresholds the system is both after one day and after three weeks still in an isotropic phase. After one day the nematic and smectic order parameter are both 0.42 and after 3 weeks the parameters are both 0.38. This means that all particles which pointing in the same direction are also positionally ordered. The low value of the order parameters is probably due to the fact that while small clusters are ordered there is no ordering between these clusters resulting in a very low order parameter, which does not give a good reflection of the sample. It does show however that the system has not yet settled. The system with 7.5 % (v/v) was so dense that it was not possible to track it. To overcome this problem we tried 3D STED microscopy in combination with the resonance mode of the confocal microscope. The rest of the settings

remained the same. We see the same happening in the system with 7.5 % (v/v) of depletant as for a volume fraction of 5 percent. The nematic order parameter is 0.26 and the smectic order parameter is 0.25 after 1 day. Again (most of) the particles are ordered in clusters which are not ordered with respect to each other.

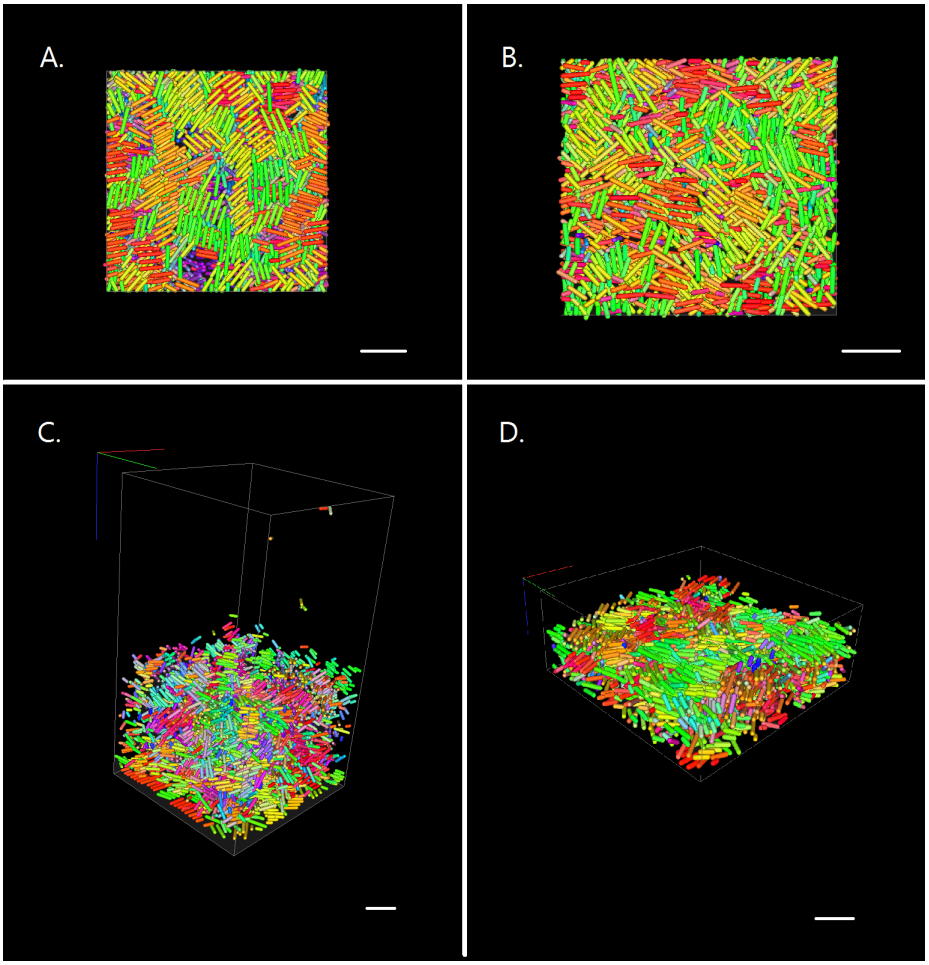

Figure 22: The computer rendered images of GD5 (A. and C.) and GW5 (B. and D.), the samples with 5.0 % (v/v) of depletant. The bottom of the sediment is shown in A. and B. and an overview of the complete z-stack is shown in C. and D. The rods are colour coded based on their orientation. All scale bars indicate 5 µm

Great differences can be found between the different samples. We see that the influence of the pressure exerted on the particles is very big. We noticed that for only 0.5 % (v/v) of depletant the order was higher halfway through the sample than at the bottom. We saw the same things for the samples containing 1 % (v/v) and 2 % (v/v) of depletant. The samples containing 5 and 7.5 % (v/v) of depletant behaved quite different, the samples seemed quite ordered but the analysis showed us that is was not. This can be explained by the ordering in small rows but no ordering between these clusters. For these samples we see that the thresholds we defined do not give a good measure of the order found in the sample, however we can say that when the

smectic and nematic order parameters are the same but both below the thresholds the system is not settled yet.

4.5.1 Difference in particle numbers between the samples after one day and after three weeks and between the different samples

All samples should constitute of the same number of particles since to every sample 100 µL of the same rod solution was added. However when looking at the z-stacks of the samples it seems this is not the case. The number of particles after 1 day and after three weeks for each sample can be seen in table 4 There are quite some differences between the different samples. Especially

Sample depletion % (v/v)	particle # after 1 day	particle # after 3 weeks
0.5	5050	2511
2	6381	7623
5	3639	2211
7.5	7768	28865

Table 4: The number of particles found in different samples after 1 day and after three weeks.

in the sample with 0.5 % (v/v) of depletant where the amount of particles has been decreased by half. This cannot be due to measuring in a different part of the sample which could be a possible explanation for the sample with 2.0 % (v/v). The most likely reason for this decrease in rods is leaking of the particles into the glue. The DMSO has reacted with the UV-glue, weakening the glue, and particles leak out of the sample. The best way to prevent this from happening is making the samples in glycerol. This means two things, one, the glue will not react with the solvent, two, the particles will move slower and it will thus be easier to image them. The combination of the slower movement of the particles together with the increased resolution of using a glycerol lens will (hopefully) result in better images and make the tracking easier and yet more accurate.

The sample of 7.5 % (v/v) shows a great increase in particle number. This is probably due to the fact that the tracking code has some difficulties tracking particles standing upright. These particles get divided intro two or three separate particles. In a sample with a lot of particles standing upright this results in a large error in the number of particles, this might be explained by a low resolution in the z direction. This is probably the cause for the large number of particles in this sample.

4.6 Dynamics

The depletant is added to create an attractive potential between the rods. But on what timescale does it have an influence? We looked at the samples with 5 % (v/v) and 7 % (v/v) of depletant in order to study this. Because of the flow in the sample it was only possible to look at the bottom of the microscope cell. Another advantage of taking this as the point of focus is that particles can enter but not leave the image. In the beginning particles are entering the plane of focus and some particles cluster together. Both the single particles and the clusters are moving around a lot. As the time passes more particles enter and after 15 minutes the first cluster of three particles has formed. As more and more particles enter the clusters get larger and they

start to move more slowly. Noticeable is that particles which are "glued" together head to tail or head to side move away from each other after some time while particles aligned side to side cannot escape from one another. This makes it possible to draw a conclusion about the strength of the depletion potential using the difference in overlap volumes.

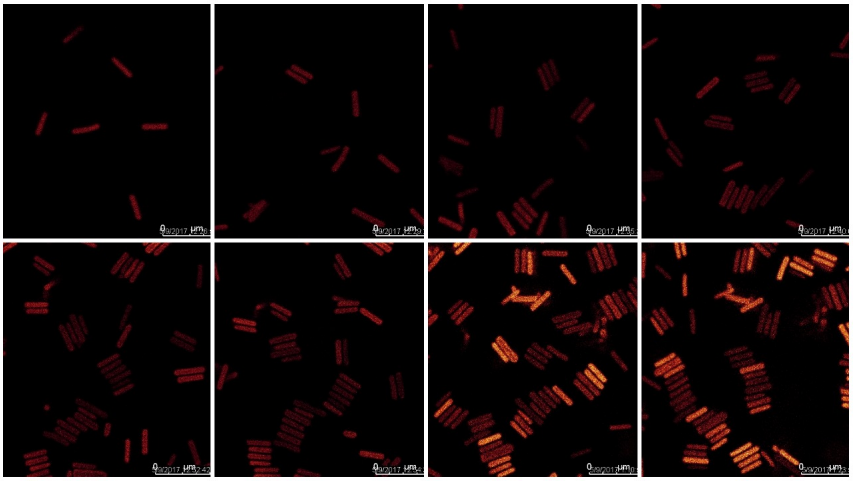

Figure 23: Images taken at the bottom of a sample of 7.5 % (v/v) depletion. All pictures have been taken at the same spot at different time intervals. From left to right, top to bottom the images have been taken after 3, 5, 10, 15, 25, 30, 45 and 60 minutes. The brighter particles are "new" in the image and have not yet lost intensity due to the laser.

In the case of 7.5 % (v/v) of depletant we see the same things happening. The first 15 minutes are similar to the system described above. But after 25 minutes the difference becomes visible, with more depletant the clusters are longer. After 90 minutes the beginning of second layer stacked on top of the bottom layer was clearly visible. Several images taken the first hour at the bottom of the sample are shown in figure 23.

5 Conclusion

The goal of this thesis was to study rod-like particles with attractive interactions on the single particle level. To do this rods and spheres were successfully synthesised. These were used to study monolayers, the monolayers learn us something about the influence of a depletant and that there exists an optimum. More depletant does not always lead to a higher order. We saw that in sediments the pressure exerted on the particles from above also plays a big role. The amount of depletant can be lowered because the pressure becomes higher. The coupling between pressure and depletant led to a strange effect. Less order was found at the bottom than at 3/4 of the sample. This might be because the particles on the bottom have so much pressure exerted on them that they are "frozen" in the clusters they formed and the beginning and need more time to settle. This while the particles higher in the sample have less pressure exerted on them and are thus freer to move. The rods try to achieve the highest possible order, to do this they must be able to settle. Again an optimum was reached, the combination of more depletant and a higher pressure do not always lead to more order. The high pressure at the bottom of the samples was no problem when considering the small sediments. Using the same depletant percentages as for the monolayers we were able to construct 3D images of the samples. By analysing these we showed quantitatively what we had already noticed qualitatively, namely that the highest order was found at 6.75 volume percent. The ultimate goal of this thesis was to track and analyse big sediments. We have studied sediments with different depletant volume fractions and imaged these after 1 day and after three weeks. We saw that only for a very low depletion potential the order increased over three weeks, as little as 2 % (v/v) was enough to make it impossible for the particles to settle in three weeks. More time would be needed to show on what timescales these particles can escape the depletion potential of a specific strength at a specific pressure.

The thresholds we defined did not give a good measure of the amount of order in a sample but did give an impression of whether the system was settled or not. Considering the dynamics of a system of rod-like particles and depletant it can be said that the clusters start forming as soon as the depletant is added. Adding more depletant makes little difference at the beginning of the settling. The clusters first grow horizontally and later also start expanding vertically. When looking real-time at the particles you can see whether head to tail/side and side tot side particles can escape from one another. This can give a measure of the strength of the depletion potential. To conclude, by making high resolution images we were able to track the rods and thus obtain the cooridinates and directions needed to analyse the samples on the single particle level. This was the main goal of this thesis and I believe this is achieved.

6 Outlook

The foundation for looking at rods acting under a depletion potential has been laid but some experiments did not go as expected. To get the right results it is important to repeat these experiments and exclude some of the possible causes of the failures. To make sure the glue will not be affected and to increase the quality of the imaging the samples must be made in glycerol instead of DMSO/water. I believe doing this will resolve most problems. When considering the gaps found in some of the samples it would be useful to look at them using the reflection mode of the confocal microscope to see exclude the posibility of drops of glue at the bottom of the samples, this is probably not the case but worth considering. Inlcuding these two enhancements to the experiments should result in correct values. It would also be nice to considering a larger amount of different depletion volume fractions to make a more accurate phase diagram.

The small sediments did not exhibit any of these problems but were made using the bigger AGF1NF4 rods, it would be nice to also make some small sediments using the smaller rods to relate them correctly to the bigger sediments.

In short, by replacing the DMSO/water with glycerol we will be sure that the glue will not leak. By using the reflection mode of the confocal microscope on the gaps we will be sure that these are no drops of glue but really formed in the sediment. And by using the smaller particles to make small sediments we will be able to relate these to the bigger sediments.

7 Acknowledgements

Ik wil Fabian graag bedanken voor alle begeleiding in het lab, achter de microscoop en met het schrijven. Zonder hem waren er nu waarschijnlijk meerdere centrifuges en microscopen kapot geweest. Daarnaast wil ik graag Arnout bedanken voor de kans om bij de SCM groep mijn bacheloronderzoek te mogen doen en de tips toen het allemaal eventjes vastliep. Alfons wil ik graag bedanken voor de tips bij de workdiscussions op vrijdagen. Chris bedankt voor de hulp met de tracking code, het installeren en uitleggen en het geven van een basis voor het schrijven van de analyse-code. Relinde bedankt voor het maken van de bolletjes, daarnaast heeft hij me geholpen met de 3DSTED. Alle studenten bij SCM bedankt voor de hulp met mathematica (vooral Michel), latex, computers en de gezelligheid.

References

[1] Manual of symbols and terminology for physicochemical quantities and units, appendix ii. *Pure Applied Chemistry*, 31, 1972.

[2] N.R. Jana, L. Gearheart, and C.J. Murphy. Seeding growth for size control of 540 nm diameter gold nanoparticles. *Langmuir*, 17:6782–6786, 2001.

[3] T.W. Ebbesen and P. M. Ajayan. Large-scale synthesis of carbon nanotubes. *Nature*, 358:220–222, 1992.

[4] J.E. Halpert, V.J. Porter, J.P. Zimmer, and M. G. Bawendi. Synthesis of cdse/cdte nanobarbells. *J. Am. Chem. Soc.*, 128:12590–12591, 2006.

[5] O. Shchepelina, V. Kozlovskaya, S. Singamaneni, E. Kharlampieva, and V.V. Tsukruk. Replication of anisotropic dispersed particulates and complex continuous templates. *J. Mater. Chem.*, 20:65876603, 2010.

[6] P. G. de Gennes. *The physics of liquid crystals.* Oxfrod university press, 1974.

[7] Thijs Besseling. *Self-assembly of colloidal spheres and rods in external fields.* Universiteit Utrecht, 2014.

[8] Jana Schwarz-Linek et al. Polymer-induced phase separation in escherichia coli suspensions. *Soft Matter*, 6:4540–4549, 2010.

[9] Yu-Jane Sheng Ssu-Wei Hu and Heng-Kwong Tsao. Depletion-induced size fractionation of nanorod dispersions. *Soft Matter*, 9:7261–7266, 2013.

[10] Zvonimir Dogic Yasheng Yang, Edward Barry and Michael F. Hagan. Self-assembly of 2d membranes from mixtures of hard rods and depleting polymers. *Soft Matter*, 8:707–714, 2012.

[11] Ahmed M. Alsayed Anna Modlińska and Thomas Gibaud. Condensation and dissolution of nematic droplets in dispersions of colloidal rods with thermo–sensitive depletants. *Scientific Reports*, 5:Article number: 18432, 2015.

[12] H.N.W. Lekkerkerker and R. Tuinier. *Colloids and the Depletion Interaction.* Springer, 2011.

[13] J. M. Perrin. *Brownian Movement and Molecular Reality.* Taylor and Francis, London, 1910.

[14] J. H. de Boer. The influence of van der waals' forces and primary bonds on binding energy, strength and orientation, with special reference to some artificial resins. *Transactions of the Faraday Society*, 32:10–37, 1936.

[15] J. N. Israelachvili. *Intermolecular and surface forces.* Academic Press, 1985.

[16] *The dielectric constant and the refractive index.* University of Cambridge, 2004-2015.

[17] Solgel department Washington. `http://depts.washington.edu/solgel/pages/courses/MSE_502/Electrostatic_Stabilization.html,picture2.18foundon31-05-2017`.

[18] E.J.W. Verwey and J. Th.G. Overbeek. *Theory of the Stability of Lyophobic Colloids.* Elsevier Publishing Company, Inc, 1948.

[19] D. Marenduzzo, K. Finan, and P.R. Cook. The depletion attraction: an underappreciated force driving cellular organization. *Journal of Cell Biology*, 175:681–686, 2006.

[20] R. Fantoni, D. Gazillo, and A. Giacometti. Phase behavior of weakly polydisperse sticky hard spheres: Perturbation theory for the percus-yevick solution. *The journal of Chemical Physics*, 125:1–2, 2006.

[21] M. Cifelli, G. Cinacchi, and L. de Geatanic. Smectic order parameters from diffusion data. *Journal of Chemical Physics*, 125:164912, 2006.

[22] Simone Dussi. *When shape is enough: from colloidal spheres to twisted polyhedra, from icosahedral to chiral order.* Universiteit Utrecht, 2016.

[23] V. Prasad, D. Semwogerere, and E.R. Weeks. Confocal microscopy of colloids. *Journal of Physics: Condensed Matter*, 19:number 11, 2007.

[24] G. B. Airy. On the diffraction of an object-glass with circular aperture. *Transactions of the Cambridge Philosophical Society*, 5:283–291, 1835.

[25] C.J.R. Sheppard and D.M. Shotton. *Confocal Laser Scanning Microscopy*. Bios scientific publishers, 1997.

[26] M. Borne and E. Wolf. *Principles of optics*. Pergamom Press, 1959.

[27] A. Kuijk, A van Blaaderen, and A Imhof. Synthesis of monodisperse, rodlike silica colloids with tunable aspect ratio. *J. Am. Chem. Soc.*, 133:2346–2349, 2011.

[28] Graz University of Technology. Fluorophores:fitc, `http://www.fluorophores.tugraz.at/substance/252`, found on 31-05-2017.

[29] W. Stöber. Controlled growth of monodisperse silica spheres in the micron size range. *Journ. Coll. Interf. Sci.*, 26:62–69, 1968.

[30] H. E. Bakker et al. Phase diagram of binary colloidal rod-sphere mixtures from a 3d real-space analysis of sedimentation-diffusion equilibria. *Soft Matter*, 12:9238–9245, 2016.

[31] Treccani L. Shahabi, S. and K. J Rezwan. Amino acid-catalyzed seed regrowth synthesis of photostable high fluorescent silica nanoparticles with tunable sizes for intracellular studies. *Journal of nanoparticle research*, 17:270., 2015.

[32] Werner Stöber and Arthur Fink. Controlled growth of monodisperse silica spheres in the micron size range. *Journal of Colloid and Interface Science*, 26:62–69, 1968.

Appendices

A Mathematica notebook

Density, Nematic and Smectic

Import data

Import the coords.rod files here. Pick a sample you want to analyse and enter the number in data=Import[files[[...]]. The number of particles, size of the sample, and a normalised 3D represantation will be given.

In[208]:=
```
files = FileNames["Z:/Users/Dido/coords.rod/*coords.rod"];
Table[{i, files[[i]]}, {i, 1, Length[files]}]
```

In[210]:=
```
data = Import[files[[5]], "Table", "FieldSeparators" → "C "];
data[[1 ;; 2]]
box = ToExpression[StringSplit[data[[2]]][[1]]
coordinaten = data[[3 ;;]];
totaal = Flatten[StringSplit[#] & /@ coordinaten, 1];
einddata =
  Table[ToExpression[StringReplace[totaal[[i]], {"e+" :→ "*10^", "e-" :→ "*10^-"}]],
   {i, 1, Length[totaal]}];
```

In[216]:=
```
pos = einddata[[All, 1 ;; 3]];
dirs = einddata[[All, 4 ;; 6]];
```

In[218]:=
```
Graphics3D[Table[{Line[{pos[[i]] + {0, 0, 0}, pos[[i]] + 3 Normalize[dirs[[i]]]}]},
  {i, 1, Length[dirs]}]]
```

Density plot

A density plot will be given, for very small samples the second command in Histogram must have a smaller value and the second command in SmoothHistogram a bigger value.

In[219]:=
```
Histogram[box[[3]] - pos[[All, 3]], 80,
 Frame → True, FrameLabel → {"z (pixels)", "# of particles"}]
SmoothHistogram[box[[3]] - pos[[All, 3]], 0.25, Frame → True,
 FrameLabel → {"z (pixels)", "Density (arb.)"}]
```

Nematic order parameter

Don’t change anything here.

In[221]:=
```
ndir = Normalize[Mean[Normalize[#] & /@ dirs]];
S = 1/Length[einddata]
  Sum[1/2 (3 (Normalize[dirs[[i]]].ndir)^2 - 1), {i, Length[einddata]}]
```

In[223]:=
```
gesorteerdopz = Sort[einddata, #1[[3]] > #2[[3]] &];
gesorteerdopz // Length
(*Sort z coordinates of particles from low 0.1 to high ~90 instead of 90 low to 0*)
gesorteerdopz[[All, 3]] = Abs[gesorteerdopz[[All, 3]] - box[[3]]];
zcoords = gesorteerdopz[[All, 3]];
```

In[227]:=
```
bins = 10;
ndirz = ConstantArray[{0, 0, 0}, bins];
For[i = 1, i ≤ Length[gesorteerdopz], i++,
 bin = Ceiling[bins * gesorteerdopz[[i, 3]] / box[[3]]];
 ndirz[[bin]] += Normalize[gesorteerdopz[[i, 4 ;; 6]]];
]
nndirz = Normalize[#] & /@ ndirz;
Svanz = ConstantArray[0, Length[gesorteerdopz]];
For[i = 1, i ≤ Length[gesorteerdopz], i++,
 bin = Ceiling[bins * gesorteerdopz[[i, 3]] / box[[3]]];
 Svanz[[i]] = 1/2 (3 (Normalize[gesorteerdopz[[i, 4 ;; 6]]].nndirz[[bin]])^2 - 1);
]
```

In[233]:=
```
ListPlot[Transpose[{zcoords, Svanz}],
 Frame → {True, True, False, False}, FrameLabel → {"z (pixels)", "S"}]
Mean[Svanz]
```

Local nematic order parameter

The local nematic order parameter in terms of z will be given. The only thing to change is the ≤ .... The number entered here is the diameter in pixels of the tracked particles.

In[235]:=
```
mat = DistanceMatrix[gesorteerdopz];
Dimensions[mat]
```

In[237]:=
```
neummat = Table[If[ mat[[k, j]] ≤ 9.2,
     Normalize[gesorteerdopz[[k, 4 ;; 6]]], Unevaluated[Sequence[]]],
   {j, 1, Length[gesorteerdopz]}, {k, 1, Length[gesorteerdopz]}];
nemdirk = (Mean[#] & /@ neummat);
```

In[239]:=
```
Slocal = 1/Length[nemdirk]
  Sum[1/2 (3 (Normalize[gesorteerdopz[[i, 4 ;; 6]]].Normalize[nemdirk[[i]]])^2 - 1),
   {i, 1, Length[neummat]}]
Snemvanz = Table[1/2
    (3 (Normalize[gesorteerdopz[[i, 4 ;; 6]]].Normalize[nemdirk[[i]]])^2 - 1),
   {i, 1, Length[neummat]}];

ListPlot[Transpose[{zcoords, Snemvanz}],
 Frame → {True, True, False, False}, FrameLabel → {"z (pixels)", "S"}]
```

Smectic order parameter

The smectic order parameter will be given. This depends upon l = the lenght of the particles in pixels, d= diameter of the particles (in pixels), and again the ≤ .... can be substituted with the diameter in pixels of the particles.

In[242]:=
```
l = 2.77/0.05;
d = 2.77/(3 * 0.05);
m = Total[Table[If[ mat[[k, j]] ≤ 9.2,  1, Unevaluated[Sequence[]]],
     {j, 1,  Length[gesorteerdopz]}, {k, 1, Length[gesorteerdopz]}], {2}];
tau = Table[ ((1/2) (3 (Normalize[gesorteerdopz[[i,  4 ;; 6]]] . Normalize[nemdirk[[i]]])^2 -
          1)) (1 - 1/m[[i]] Sum[ ((dirs[[i]] - dirs[[j]]) . Normalize[nemdirk[[i]]])/((1 + d)/2), {j, 1, m[[i]]}]),
    {i, 1, Length[gesorteerdopz]}];
```

In[246]:=
```
ListPlot[Transpose[{zcoords, tau}],
 Frame → {True, True, False, False}, FrameLabel → {"z  (pixels)", "τ" }]
Mean[
 tau]
```

Pressure profile

In[248]:=
```
lm = 2653 * 10^-9;
dm = 623 * 10^-9;
vol =  Pi (dm/2)^2 * lm;
rho = 2;
g = 9.81;
np = StringReplace[data[[1]], {"&" :→  ""}];
Druk =
  Table[ ((Length[gesorteerdopz] - i) * vol * g * rho) / (dm * lm) / (1.38 * 10^-23 * 272) * (dm)^3,
   {i, 1, Length[gesorteerdopz]}];
```

In[255]:=
```
ListPlot[Transpose[{zcoords, Druk}],
 Frame → {True, True, False, False}, FrameLabel → {"z", "βPD^3" }]
```

B Microscope settings